Image reconstruction for fluorescence tomography

Marina Chukalina

Institute of Microelectronics Technology and High Purity Materials RAS

Chernogolovka, Russia

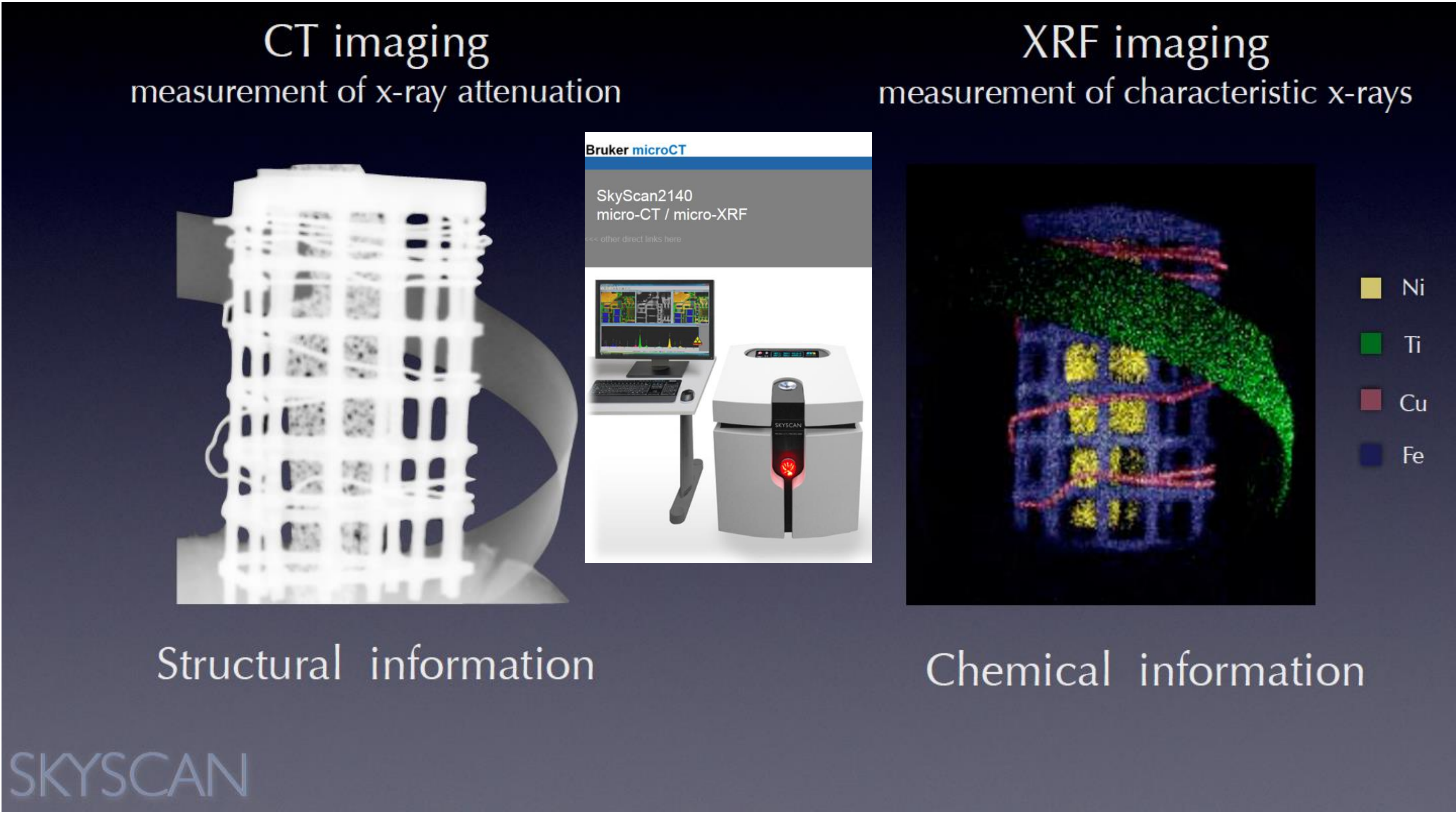
CT imaging
measurement of x-ray attenuation
XRF imaging
measurement of characteristic x-rays
Bruker microCT
SkyScan2140
micro-CT / micro-XRF
Ni
Ti
Cu
Fe
Structural information
Chemical information
SKYSCAN

Sr distribution in rat vertebra

CT

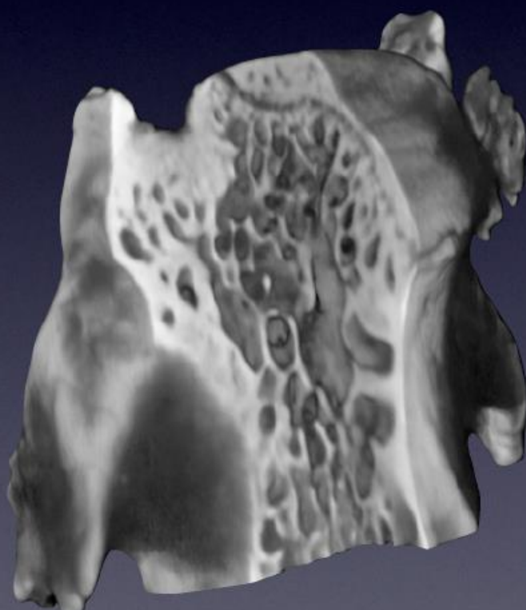

CT+XRF

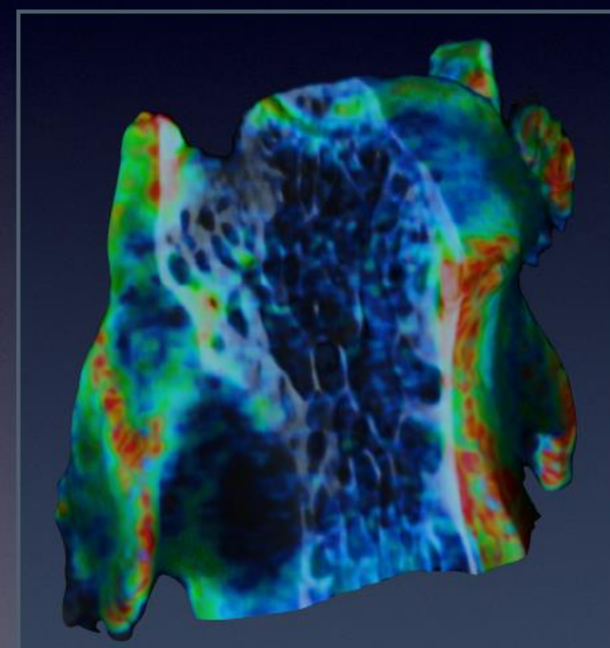

OUTLINE

- Sinogram formation
- Different set-ups:
  microbeam, pihnole, confocal
- Fast core for calculations

SETUP: CLASSICAL SCHEME

YUASA *et al.*: FLUORESCENT X-RAY COMPUTED TOMOGRAPHY

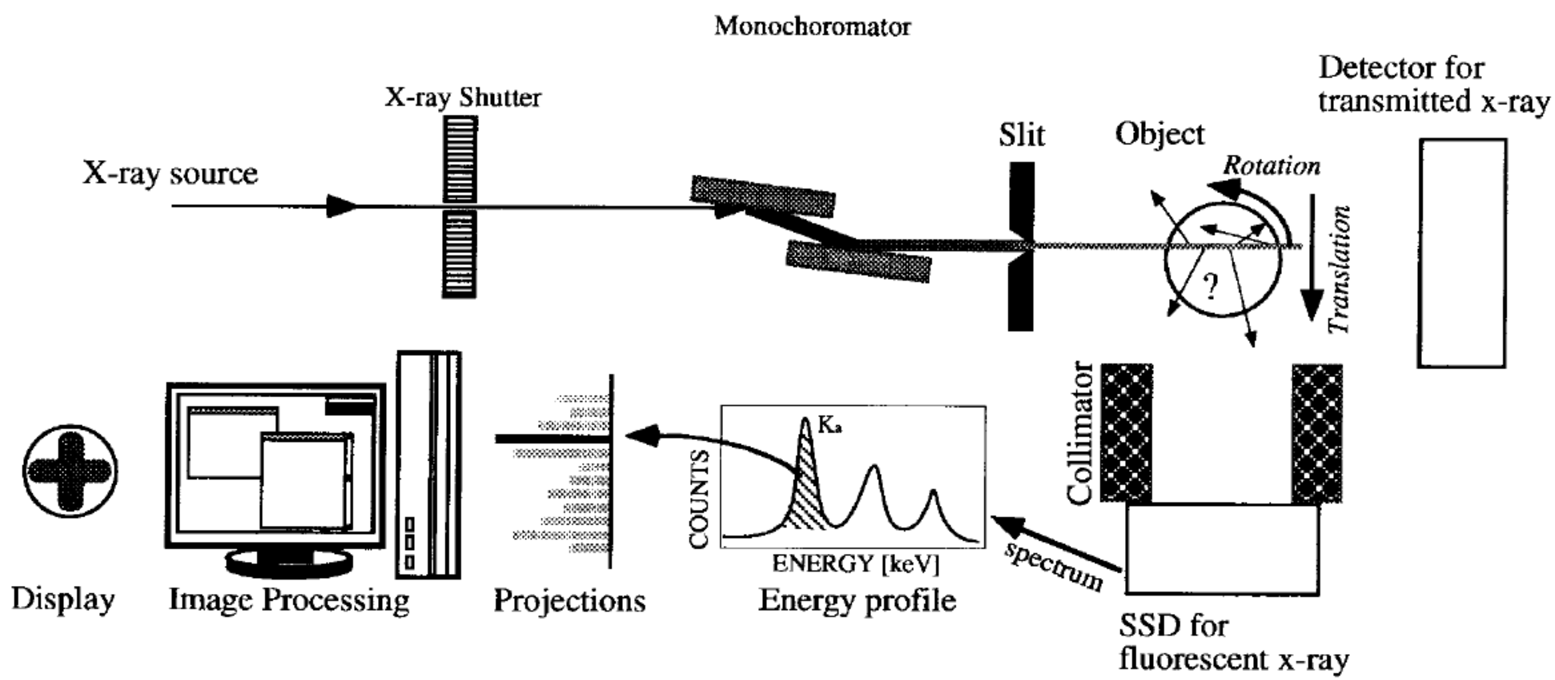

Fig. 1. Schematic diagram of a typical FXCT experimental system.

IEEE TRANSACTIONS ON NUCLEAR SCIENCE, VOL. 44, NO. 1, FEBRUARY 1997

Reconstruction Method for Fluorescent X-Ray Computed Tomography by Least-Squares Method Using Singular Value Decomposition

Tetsuya Yuasa, Masahiro Akiba, Tohoru Takeda, Masahiro Kazama, Atsunori Hoshino, Yuki Watanabe, Kazuyuki Hyodo, F. Avraham Dilmanian, Takao Akatsuka, and Yuji Itai

COORDINATE SYSTEMS

$$s = x \cos\alpha + y \sin\alpha$$
$$t = -x \sin\alpha + y \cos\alpha.$$

- Q is an elementary volume
- The volume contains an ensemble of elements
- Quantitative description of ensemble member *is*

$$\rho(s, t', i)$$

- Each member is determined unique by Z (atomic number)

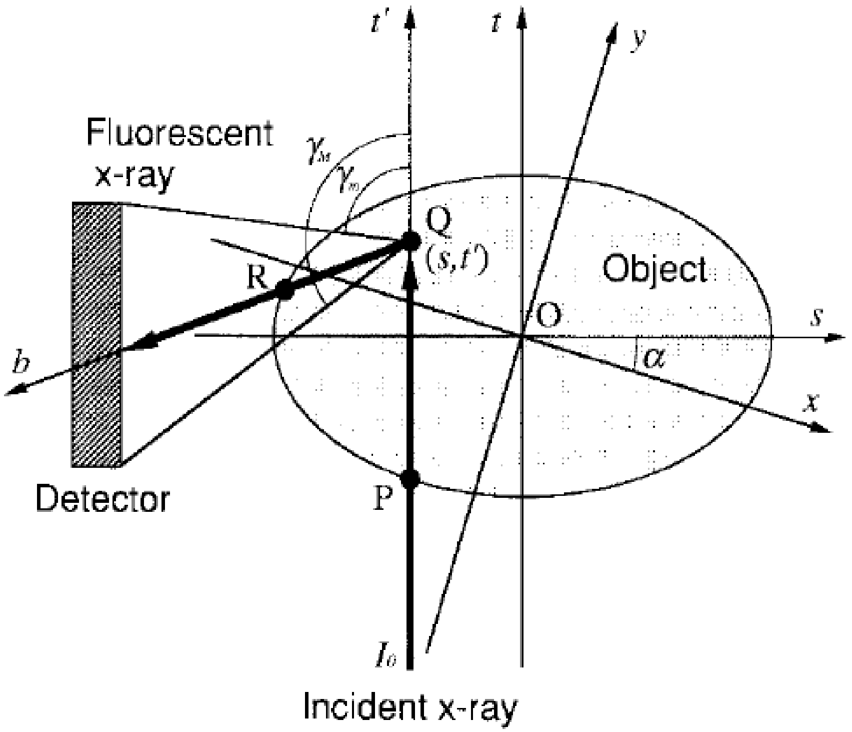

Model of the volume in element terms:

- $\sum_1^M \rho(s, t', i) = 1$
- M is determined by registered spectra

But element has emission spectrum not ONE energy line!

PROJECTION. From spectrum to element

Model of the volume in element terms:

- $\sum_1^M \rho(s,t',i) = 1$
- M is determined by registered spectra

ith element gives spectrum

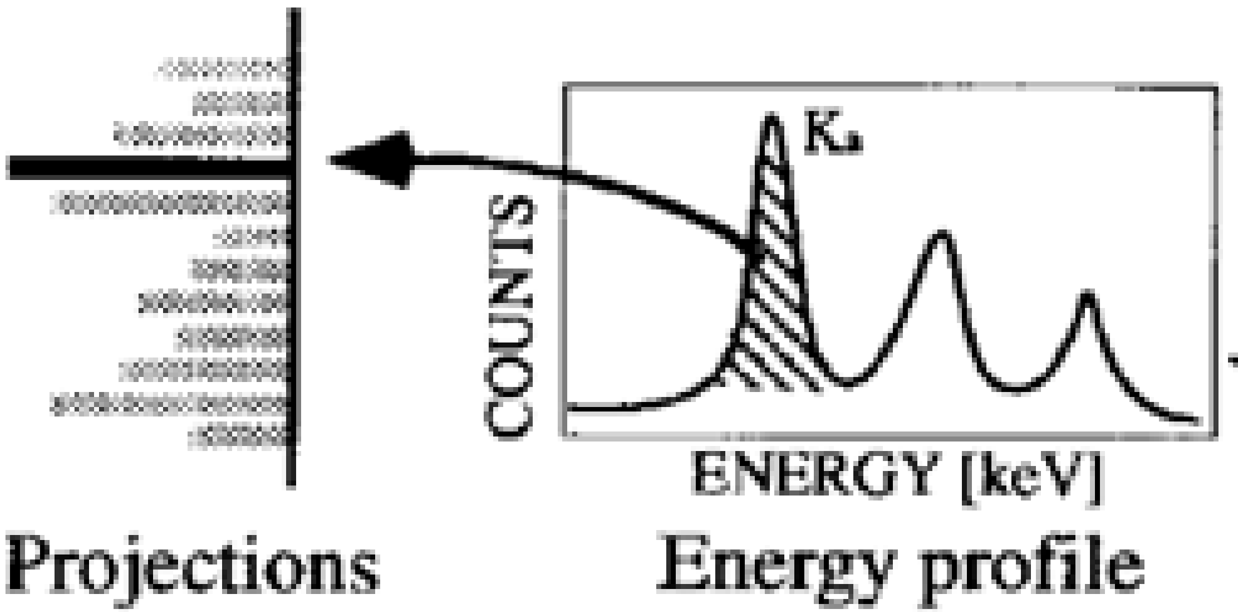

Model:
ith energy channel of detector = chemical element Z_i (E_i)
chemical element Z_i = most intensive characteristic line of ith element
Number of channels is more then number of elements
Later we will take full element spectrum into account

PROBLEM STATEMENT

• To reconstruct
vector image from vector sinogram

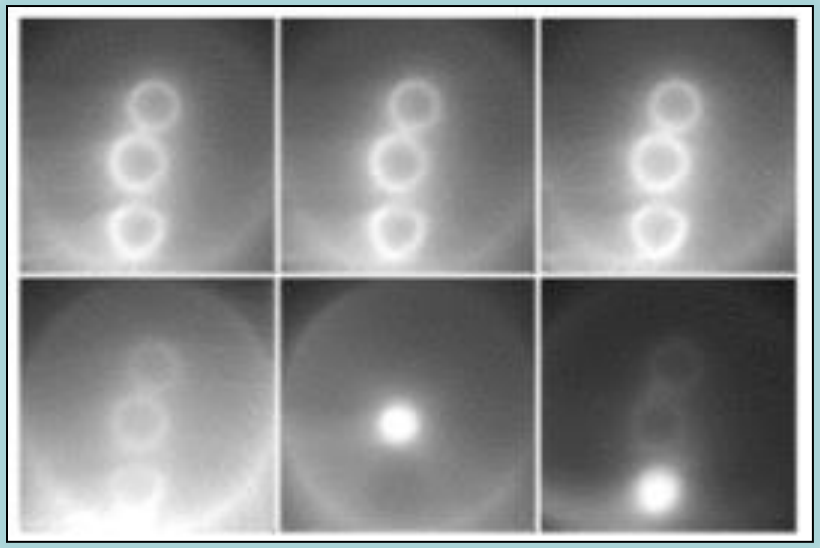

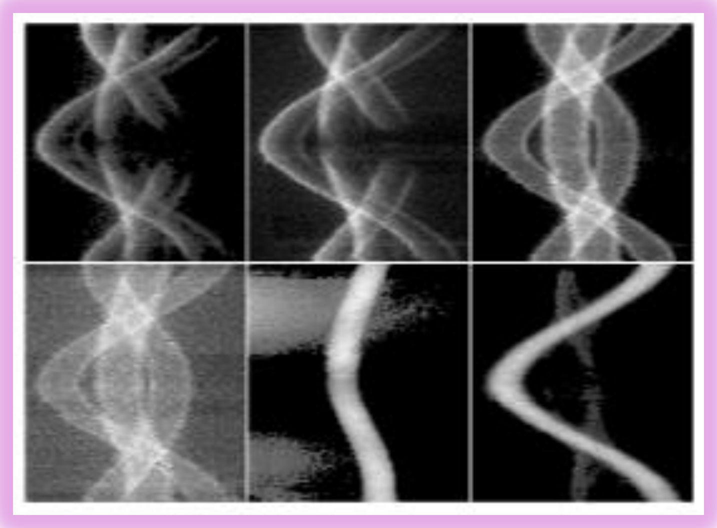

Sinograms of sample 1 (left to right, top to bottom)
Ba-Lα and Ba-Lβ, Sr-Kα, Zr-Kα, Cu-Kα, As-Kα

- Vector coordinate is description of the ensemble element (density, weight fraction, number of atoms…)

We collect $I_{fl}(\, s, \alpha, E_0, E_i)$

(s, α) - position of X-ray beam , rotation angle
E_0 - incident beam energy
E_i - energy for element Z

$$s = x \cos\alpha + y \sin\alpha$$
$$t = -x \sin\alpha + y \cos\alpha.$$

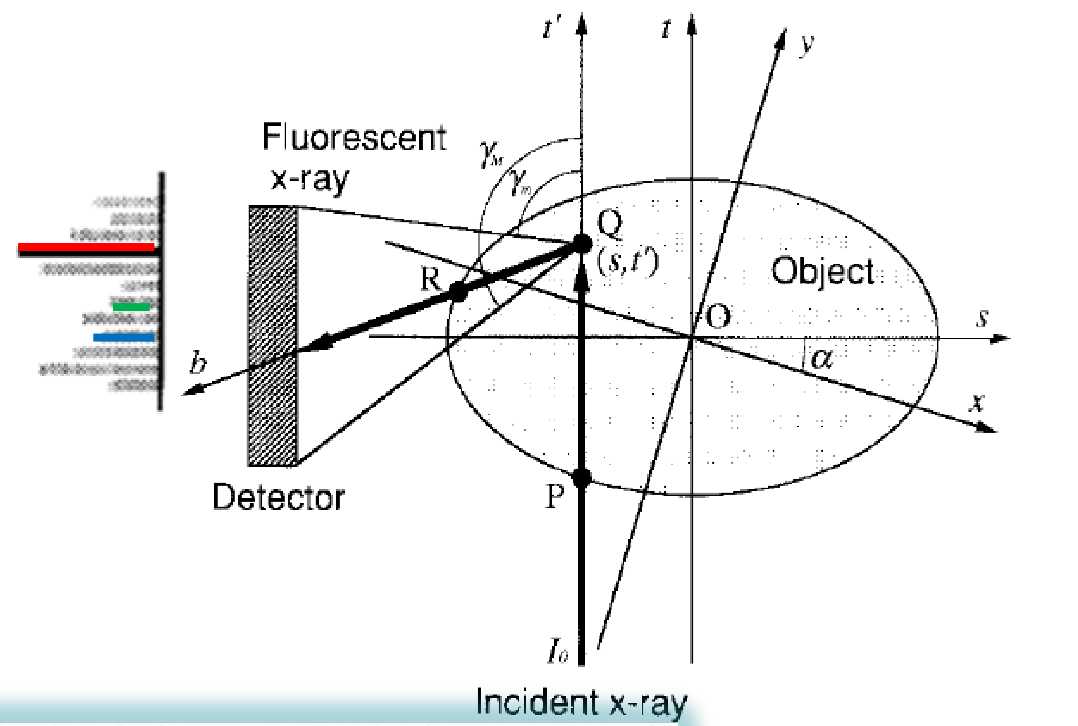

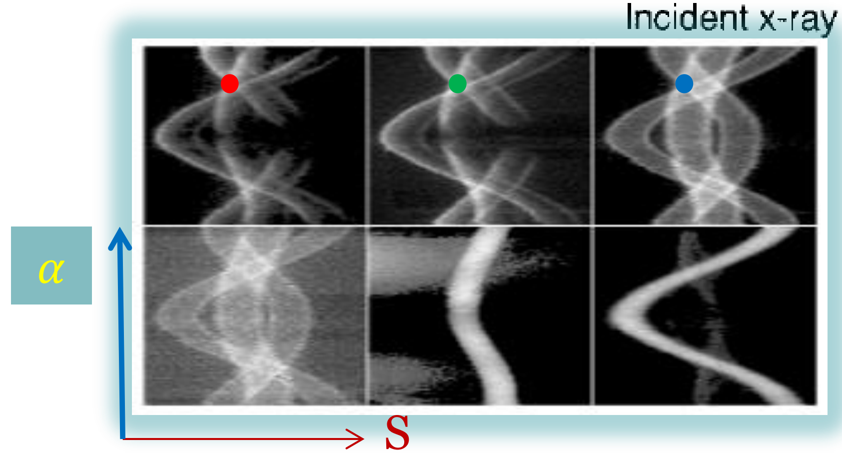

$$s = x \cos\alpha + y \sin\alpha$$
$$t = -x \sin\alpha + y \cos\alpha.$$

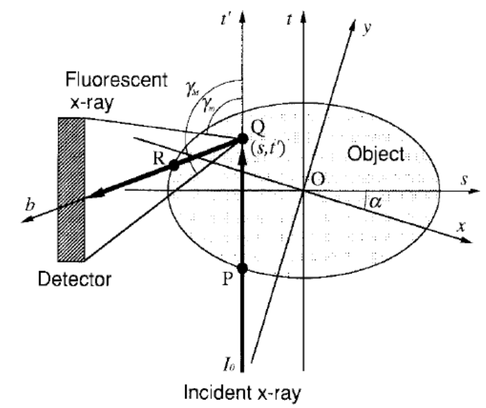

Fig. 2. Coordinate systems for FXCT.

1. X-ray flux rate reaching the point **Q**

$$I(s,t',E_0)=I_0 exp\left[-\int_0^{t'}\mu_0(s,t)dt\right]$$

2. The flux rate of the fluorescent X-ray $\boldsymbol{E_i}$ emitted from the point **Q to detector** direction

$$I_2(s,t',E_i,E_0) = K(E_0,i)\rho(s,t',i)I_0 exp\left[-\int_0^{t'}\mu_0(s,t)dt\right]\Delta t'$$

$$if\,\rho \text{ is } density \text{ then } K(E_0,i) = \frac{N_A\sigma(i,E_0)}{A_r(i)}$$

N_A - Avagadro's number
$\sigma(i,E_0)$ - cross-section of fluorescence
$A_r(i)$ - relative atomic mass

3. Following a single ray among fluorescent X-rays emitted from **Q**

$$I_3(s,t',E_i,E_0) = I_2(s,t',E_i,E_0)\cdot \exp\left[-\int_0^{\infty}\mu_i(s-b\cos\gamma, s+b\sin\gamma)\,db\right]$$

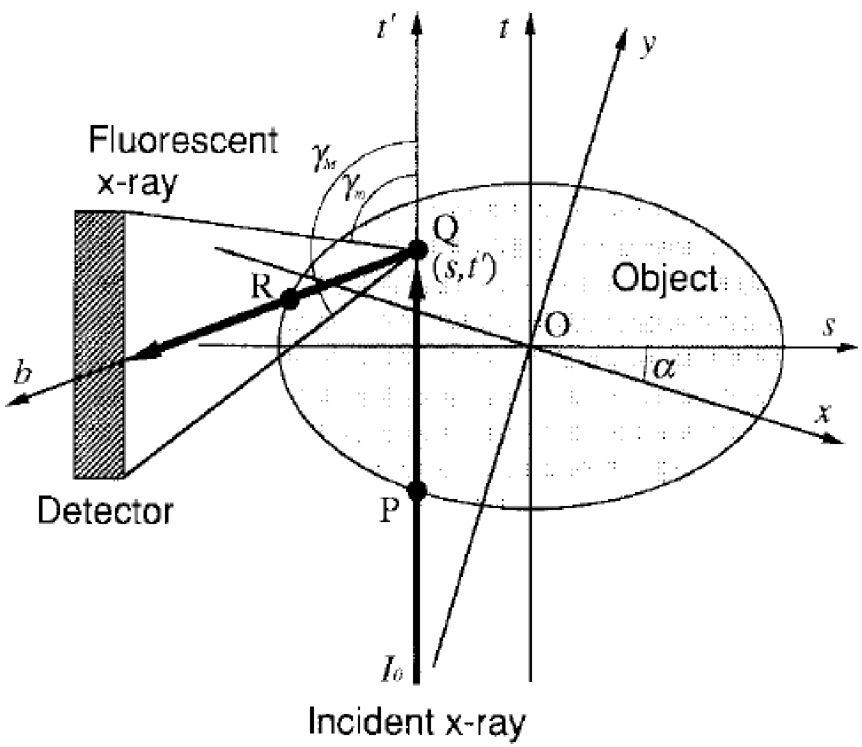

$$s = x\cos\alpha + y\sin\alpha$$
$$t = -x\sin\alpha + y\cos\alpha.$$

Fig. 2. Coordinate systems for FXCT.

4. Flux rate of the fluorescent X-ray emitted from ***Q*** and detected

$$I_4(s,t',E_i,E_0) = I_2(s,t',E_i,E_0)\int_{\gamma_m}^{\gamma_M} exp\left[-\int_0^{\infty}\mu_i(s-bcos\gamma, s+bsin\gamma)db\right]d\gamma$$

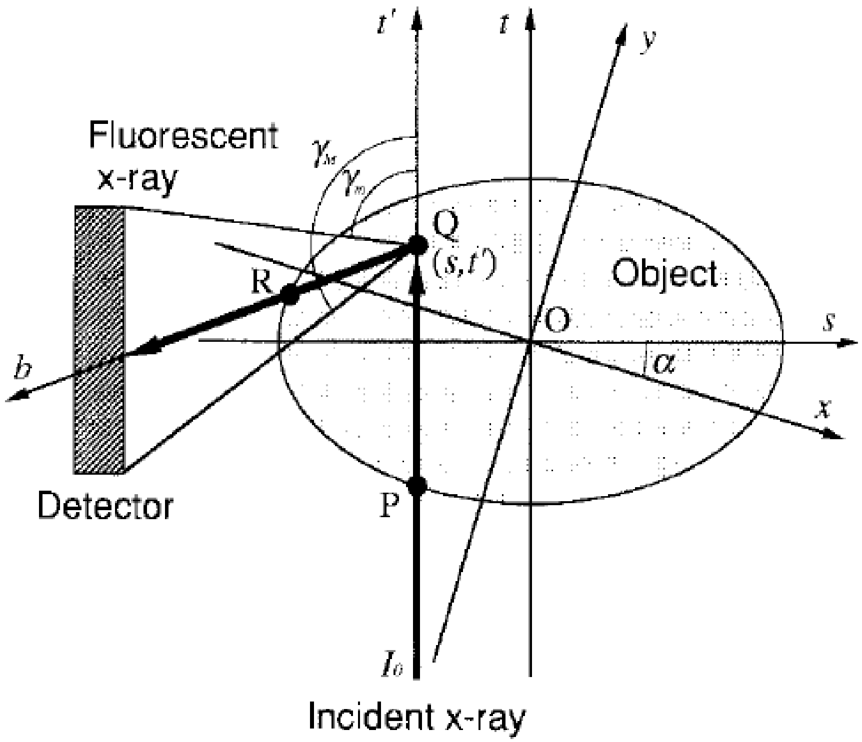

$$s = x\cos\alpha + y\sin\alpha$$
$$t = -x\sin\alpha + y\cos\alpha.$$

Fig. 2. Coordinate systems for FXCT.

5. Total flux rate of the fluorescent X-ray reaching the detector for an incident X-ray

$$I_{fl}(s,\alpha,E_i,E_0) = \int_{-\infty}^{\infty} I_2(s,t',E_i,E_0) \int_{\gamma_m}^{\gamma_M} exp\left[-\int_0^{\infty} \mu_i(s-b\cos\gamma, s+b\sin\gamma)db\right] d\gamma\, dt'$$

$$I_2(s,t',E_i,E_0) = K(E_0,i)\rho(s,t',i)I_0 exp\left[-\int_0^{t'} \mu_0(s,t)dt\right]\Delta t'$$

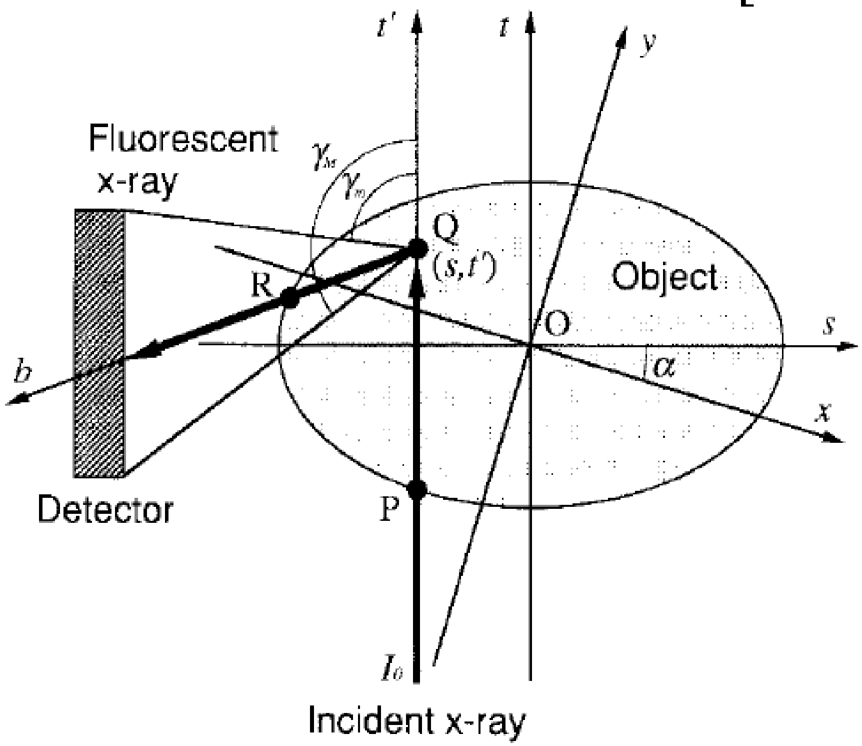

$$s = x\cos\alpha + y\sin\alpha$$

$$t = -x\sin\alpha + y\cos\alpha.$$

Fig. 2. Coordinate systems for FXCT.

If we neglect attenuation of fluorescence then we have the problem like CT problem

$$I_{fl}(s,\alpha,E_i,E_0) = \int_{-\infty}^{\infty} I_2(s,t',E_i,E_0)\,\cancel{\int_{\gamma_m}^{\gamma_M} exp\left[-\int_0^{\infty}\mu_i(s-b\cos\gamma,s+b\sin\gamma)db\right] d\gamma}\, dt'$$

$$I_2(s,t',E_i,E_0) = K(E_0,i)\rho(s,t',i)I_0 exp\left[-\int_0^{t'}\mu_0(s,t)dt\right]\Delta t'$$

$RT[I_2(x,y)]$

$$\boldsymbol{I_{fl}}(s,\alpha,E_i,E_0) = \int_{-\infty}^{\infty} \boldsymbol{I_2}(s,t',E_i,E_0)\,dt'$$

If in addition we neglect attenuation of incident beam we have the problem like CT problem

$$I_{fl}(s,\alpha,E_i,E_0)=\int_{-\infty}^{\infty} K(E_0,i)\rho(s,t',i)I_0\cancel{exp\left[-\int_0^{t'}\mu_0(s,t)dt\right]}dt'$$

$RT[\hat{\rho}(x,y,i)K(E_0,i)]$

$$I_{fl}(s,\alpha,E_i,E_0)=I_0\int_{-\infty}^{\infty} K(E_0,i)\rho(s,t',i)dt'$$

$$K(E_0,i)=\frac{N_A\sigma(i,E_0)}{A_r(i)}$$

TO INVERSE PROBLEM

$$RT[I_2(x,y)]$$

$$RT[\hat{\rho}(x,y,i)K(E_0,i)]$$

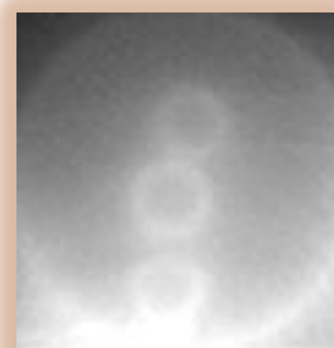

We would like to reconstruct $\rho(x,y,i)$

$$I_{fl}(s,\alpha,E_i,E_0) =$$

$$\int_{\gamma_m}^{\gamma_M}\int_{-\infty}^{\infty} K(E_0,i)\rho(s,t',i)I_0 exp\left[-\int_0^{t'}\mu_0(s,t)dt\right] exp\left[-\int_0^{\infty}\mu_i(s-bcos\gamma, s+bsin\gamma)db\right]d\gamma\, dt'$$

$$\mu_0 = \sum_j \rho_j \mu_{0j}^m \qquad \mu_i = \sum_j \rho_j \mu_{ij}^m$$

$$I_{fl}(s,\alpha,E_i,E_0\,)=\int_{\gamma_m}^{\gamma_M}\int_{-\infty}^{\infty}exp\left[\log F_1(\rho)-\int F_2(\rho)-\int F_3(\rho)\right]d\gamma\,dt'$$

$$I_{fl}(s,\alpha,E_i,E_0\,)=$$
$$\int_{\gamma_m}^{\gamma_M}\int_{-\infty}^{\infty}exp[\log(K(E_0,i)\rho(s,t',i)I_0)]exp\left[-\int_0^{t'}\mu_0(s,t)dt\right]exp\left[-\int_0^{\infty}\mu_i(s-bcos\gamma,s+bsin\gamma)db\right]d\gamma\,dt'$$

We would like to reconstruct $\rho(x,y,i)$

$$I_{fl}(s,\alpha,E_i,E_0\,)=$$
$$\int_{\gamma_m}^{\gamma_M}\int_{-\infty}^{\infty}K(E_0,i)\rho(s,t',i)I_0exp\left[-\int_0^{t'}\mu_0(s,t)dt\right]exp\left[-\int_0^{\infty}\mu_i(s-bcos\gamma,s+bsin\gamma)db\right]d\gamma\,dt'$$

$$\mu_0=\sum_j\rho_j\mu_{0j}^m \qquad \mu_i=\sum_j\rho_j\mu_{ij}^m$$

$$I_{fl}(s,\alpha,E_i,E_0)/I_0 = \cancel{\int_{\gamma_m}^{\gamma_M}\int_{-\infty}^{\infty}} exp\left[\log F_1(\rho) - \int F_2(\rho) - \int F_3(\rho)\right] d\gamma\, dt'$$

Solution by set-up

$$I_{fl}(s,\alpha,E_i,E_0)/I_0 = exp\left[\log F_1(\rho) - \int F_2(\rho) - \int F_3(\rho)\right]$$

$$\log(I_{fl}(s,\alpha,E_i,E_0)/I_0) = \log F_1(\rho) - \int F_2(\rho) - \int F_3(\rho)$$

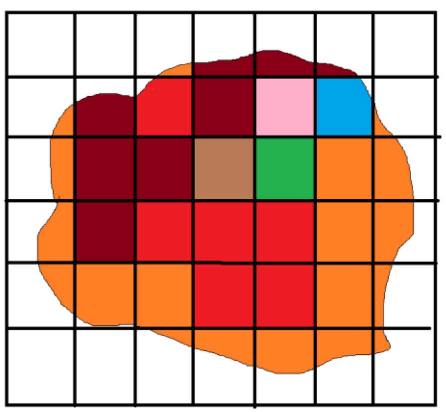

$\log(F_1)$
*k*th iteration

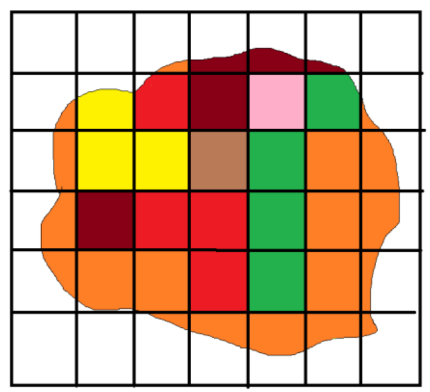

F_2
from CT

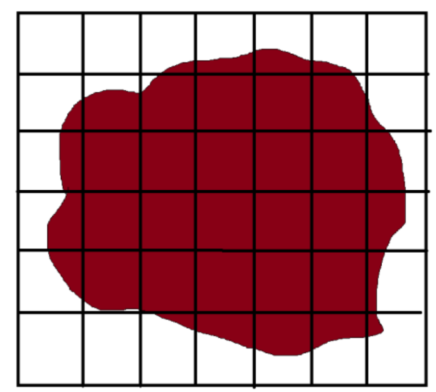

F_3
*(k-1)*th iteration

SET-UP: CONFOCAL COLLIMATORS

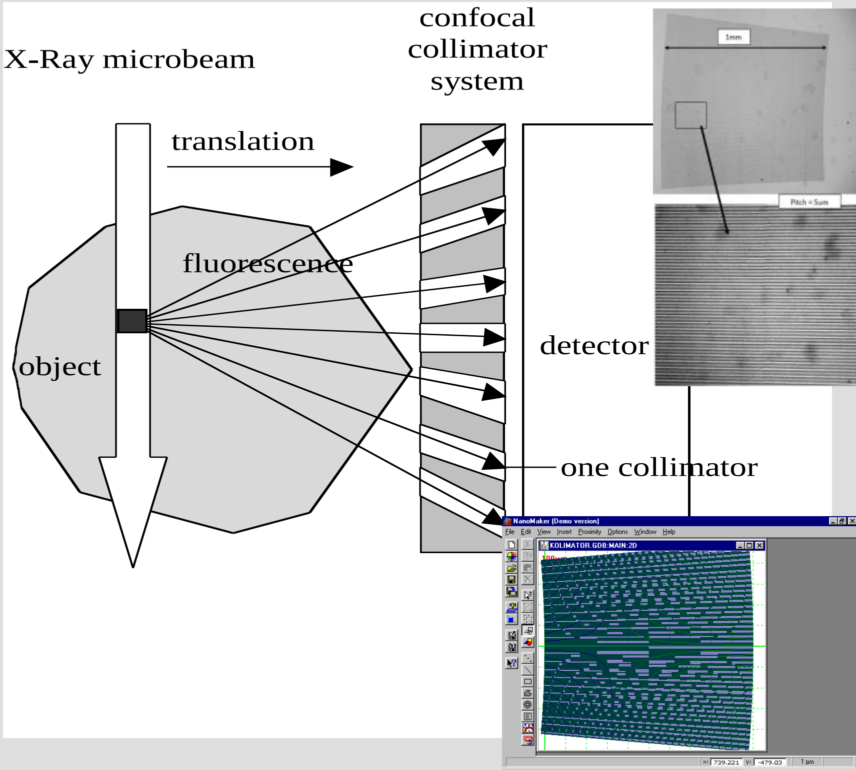

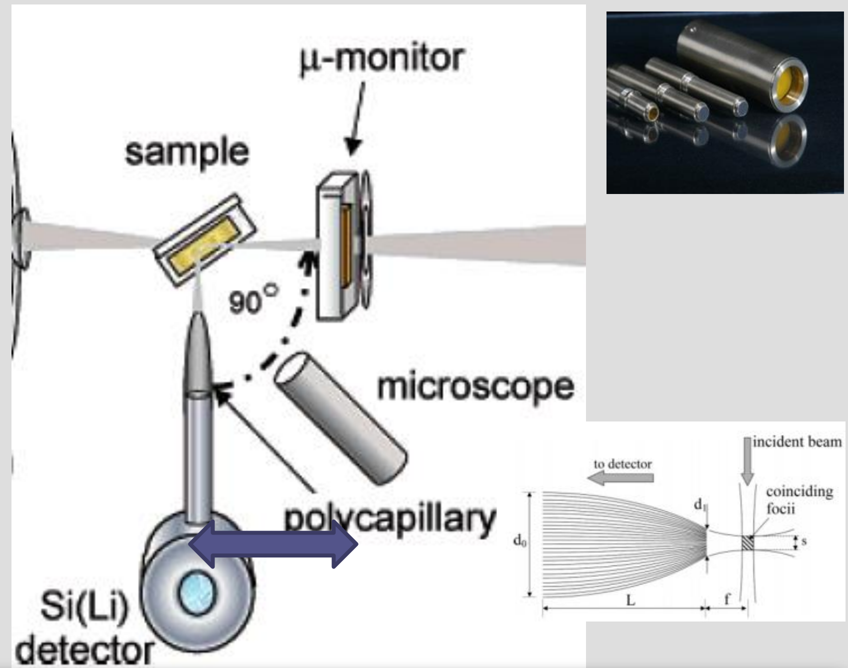

M. Chukalina, A. Simionovici, S. Zaitsev. X-ray fluorescence microtomography comparison between a standart CT setup and a confocal collimator apparatus. Proceedings of the X-ray Optics Workshop. Nizhnii Novgorod, Russia. May 2-6 (2004)261-265.

Anal. Chem. **2004**, *76*, 6786–6791

Three-Dimensional Trace Element Analysis by Confocal X-ray Microfluorescence Imaging

Laszlo Vincze,*,† Bart Vekemans,† Frank E. Brenker,‡ Gerald Falkenberg,§ Karen Rickers,§,∥ Andrea Somogyi,⊥ Michael Kersten,# and Freddy Adams†

$$I_{fl}(s,\alpha,E_i,E_0\ ) = \int_{\gamma_m}^{\gamma_M} \cancel{\int_{-\infty}^{\infty}} exp\left[\log F_1(\rho) - \int F_2(\rho) - \int F_3(\rho)\right] d\gamma\, dt'$$

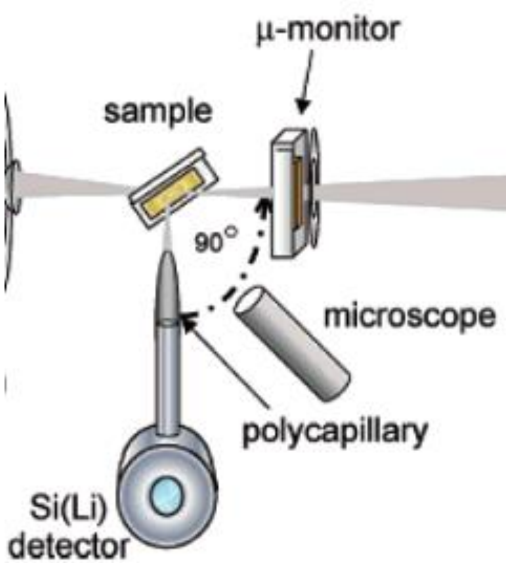

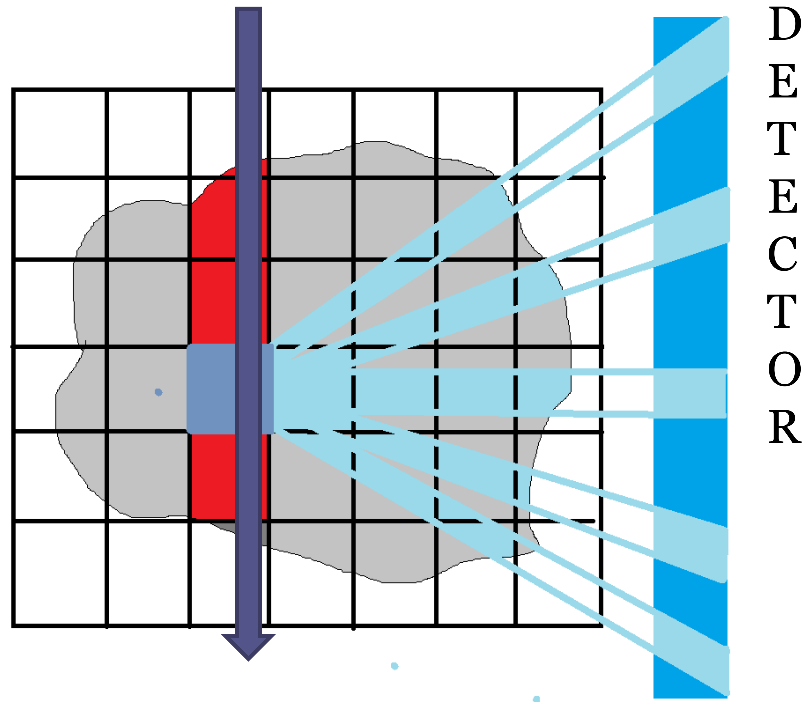

$$I_{fl}(s,\alpha,E_i,E_0\ ) = \cancel{\int_{\gamma_m}^{\gamma_M}} \cancel{\int_{-\infty}^{\infty}} exp\left[\log g F_1(\rho) - \int F_2(\rho) - \int F_3(\rho)\right] d\gamma\, dt'$$

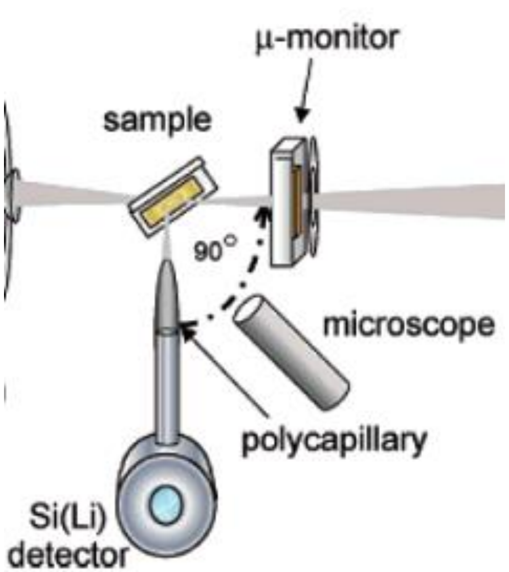

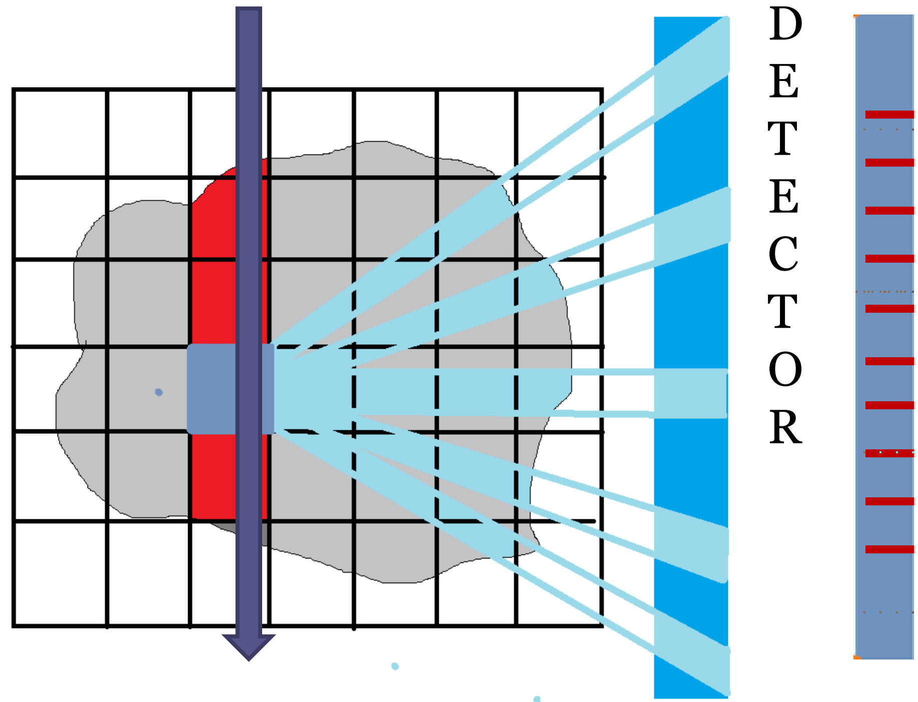

COLLECTION FUNCTION III

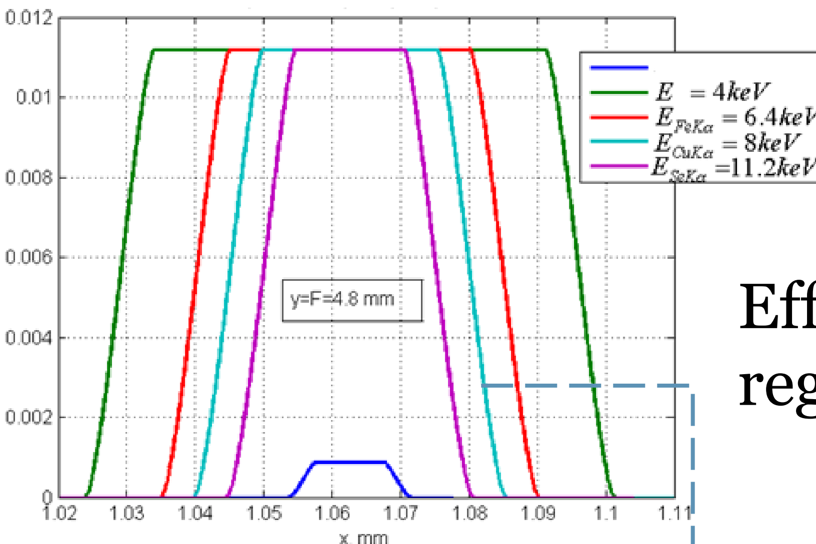

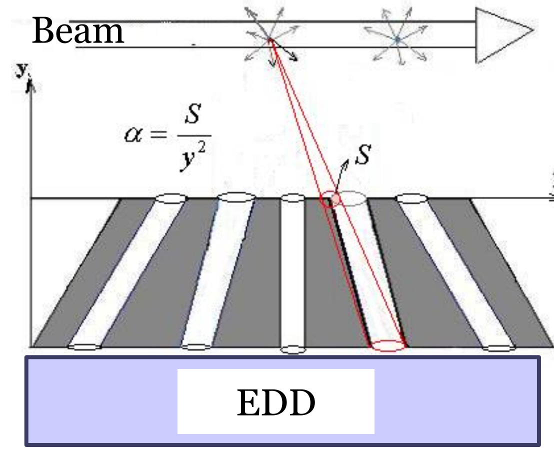

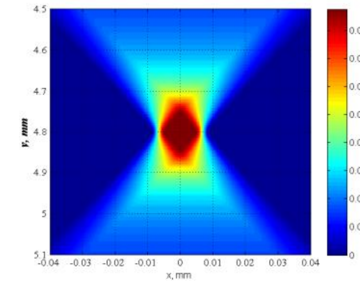

Effective collection region (ECR)

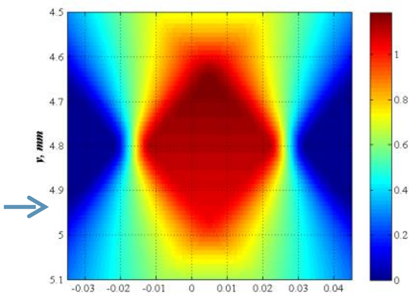

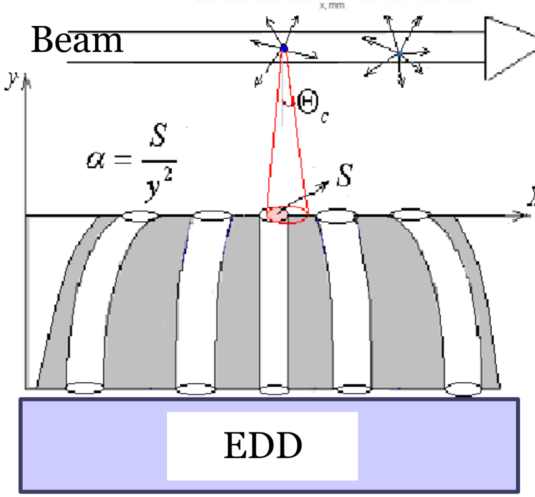

$\theta_c(E)!$

$$F(x,y,z,E) = \frac{I_c(x,y,z,E)}{I_g(x,y,z,E)} \sim \sum_i \alpha_i$$

Focal volume is an intersection of ECR with illuminated part of the sample

SET-UP: PINHOLE IMAGING PRINCIPLE

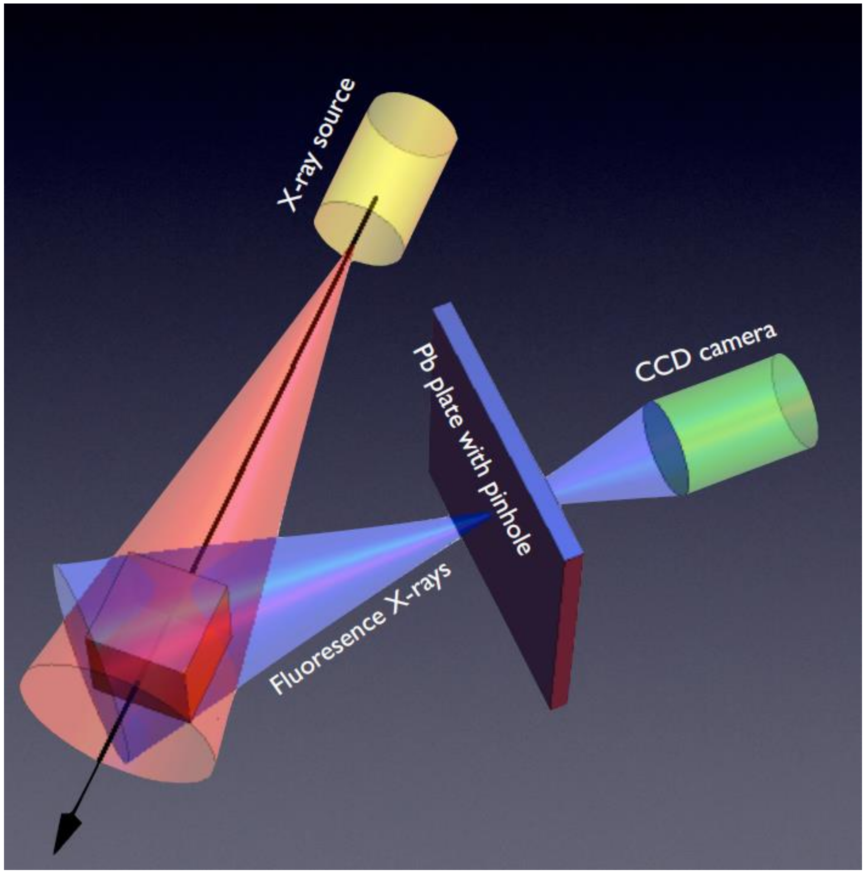

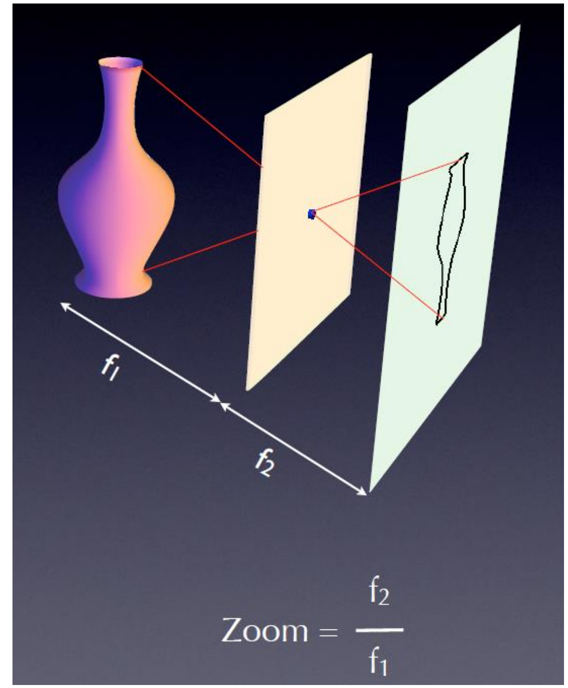

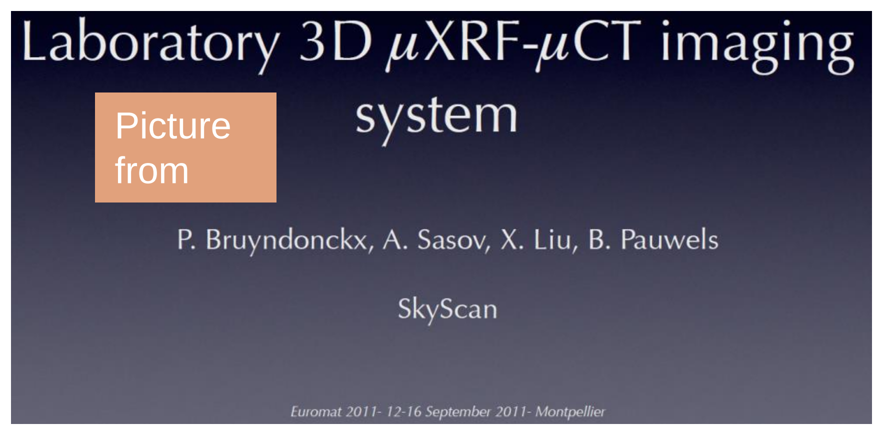

$$I_{fl}(s,\alpha,E_i,E_0\,) = \int_{\gamma_m}^{\gamma_M} \cancel{\int_{-\infty}^{\infty}} exp\left[\log F_1(\rho) - \int F_2(\rho) - \int F_3(\rho)\right] d\gamma\, dt'$$

$\int$

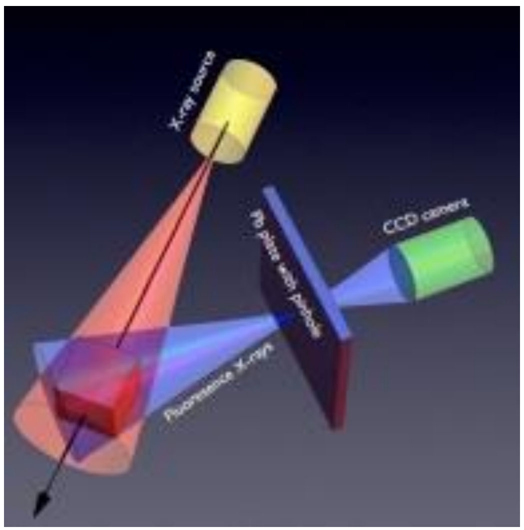

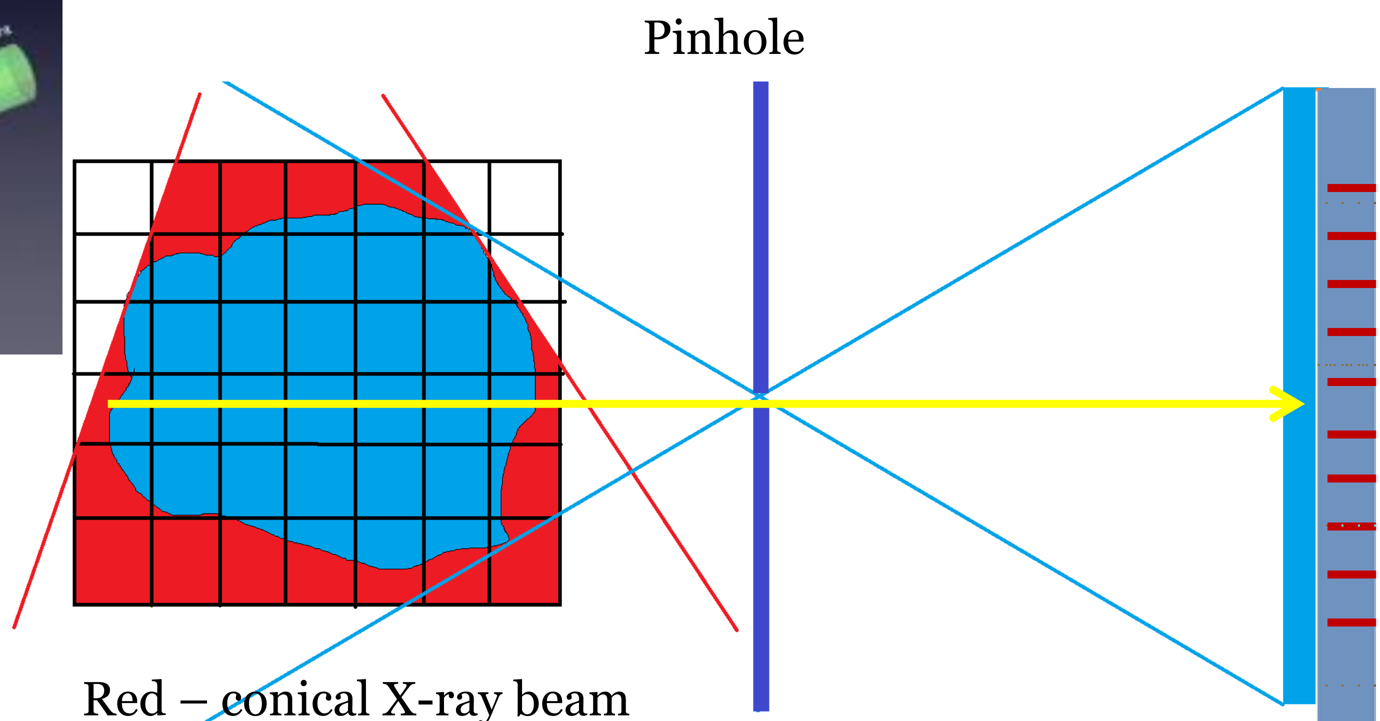

$$I_{fl}(s,\alpha,E_i,E_0) = \int_{\gamma_m}^{\gamma_M} \int_{-\infty}^{\infty} exp\left[\log F_1(\rho) - \int F_2(\rho) - \int F_3(\rho)\right] d\gamma\, dt'$$

YUASA *et al.*: FLUORESCENT X-RAY COMPUTED TOMOGRAPHY

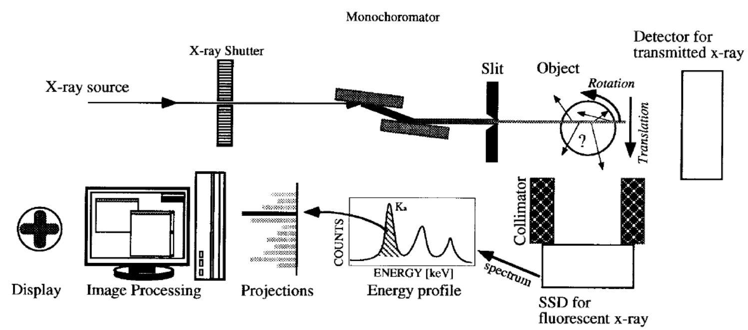

Fig. 1. Schematic diagram of a typical FXCT experimental system.

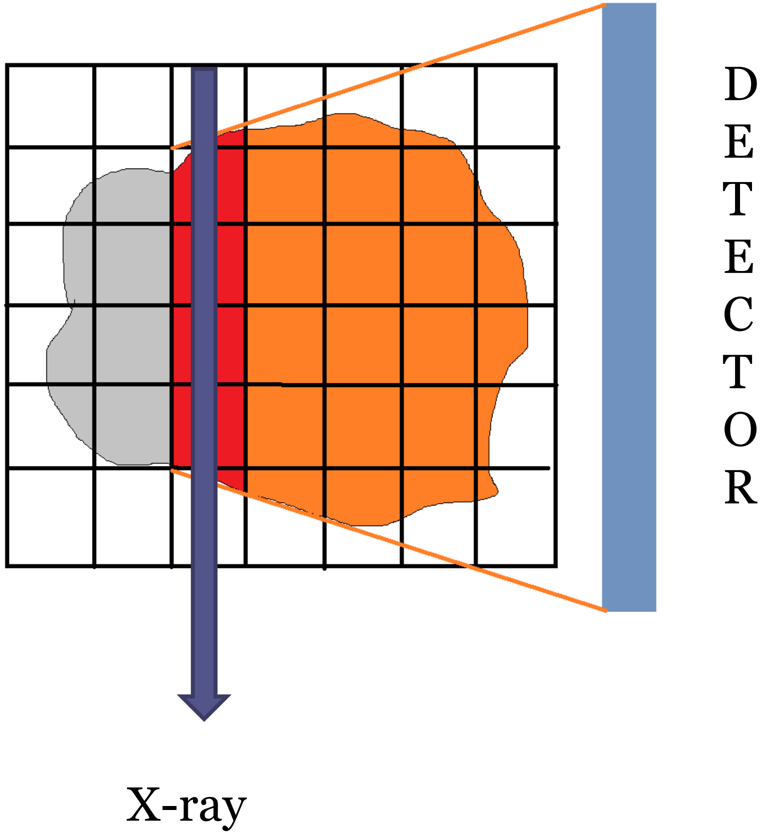

$$I_{fl}(s,\alpha,E_i,E_0\,)=\int_{\gamma_m}^{\gamma_M}\int_{-\infty}^{\infty}exp\left[\log F_1(\rho)-\int F_2(\rho)-\int F_3(\rho)\right]d\gamma\, dt'$$

YUASA *et al.*: FLUORESCENT X-RAY COMPUTED TOMOGRAPHY

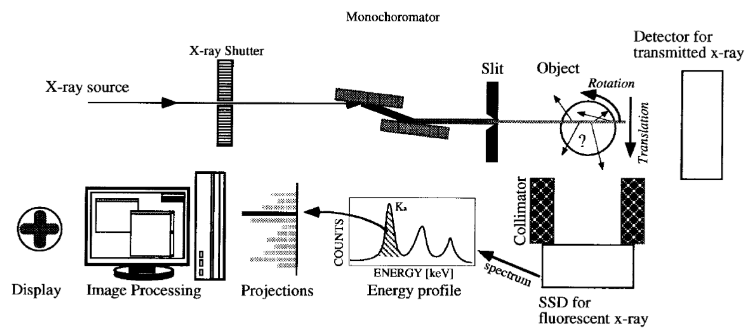

Fig. 1. Schematic diagram of a typical FXCT experimental system.

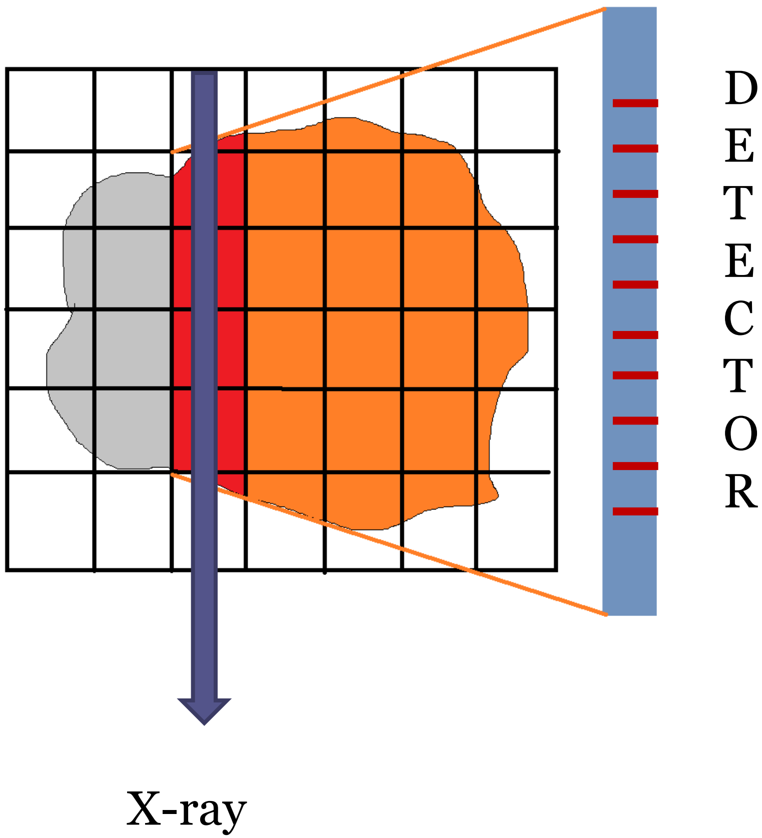

$$I_{fl}(s, \alpha, E_i, E_0)/I_0 = \int_{\gamma_m}^{\gamma_M} \int_{-\infty}^{\infty} exp\left[\log F_1(\rho) - \int F_2(\rho) - \int F_3(\rho)\right] d\gamma\, dt'$$

No easy way to deduce problem to the linear one was found for 17 years

However, nonlinear systems can be solved directly numerically by optimization methods (direct methods like pattern search or common 1st order methods like gradient descend)

WHAT WE ARE DOING:

FBP	SART	SART + FHT
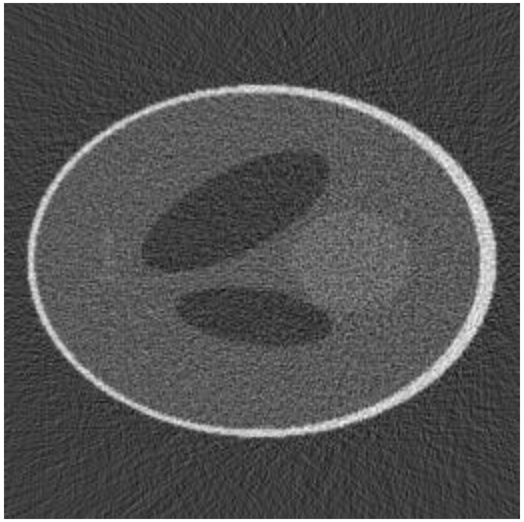	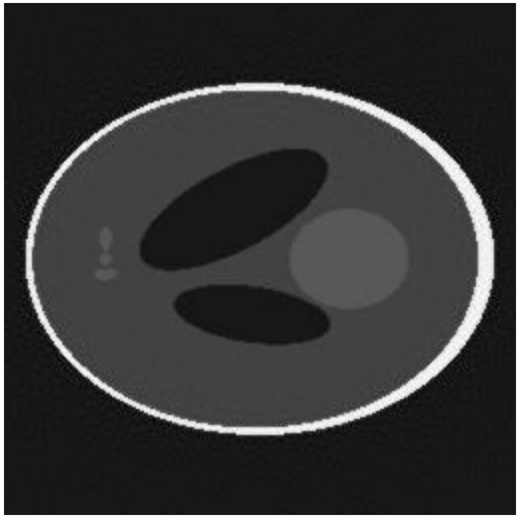	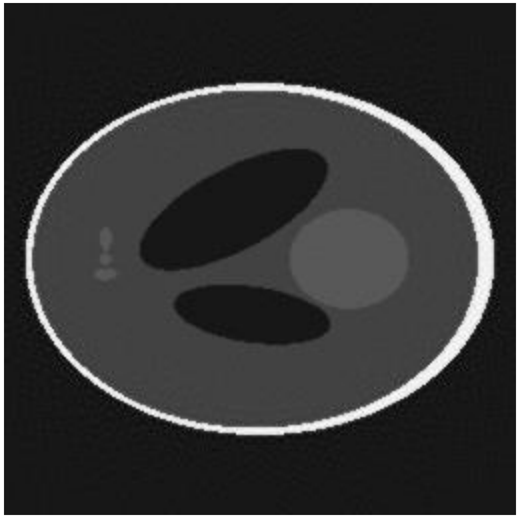
$O(n^2 \log n)$	$O(n^3)$	$O(n^2 \log n)$

FAST HOUGH TRANSFORM

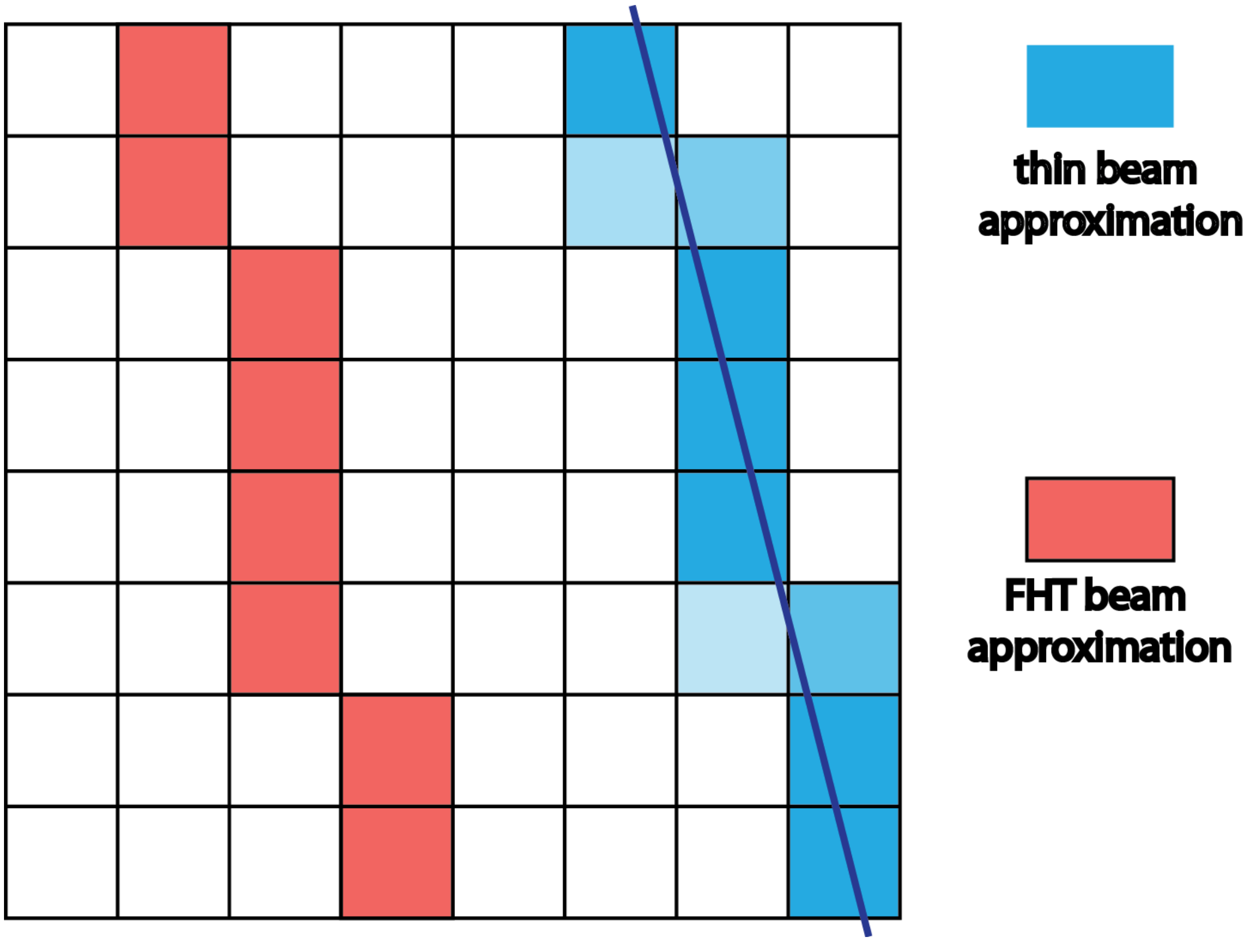

Number of different FHT angle patterns for nxn image ≈ 4n

FHT of an NxN image can be calculated with O(n^2log n) operations [3]

Nikolaev D., Karpenko S., Nikolaev I., Nikolayev P, 2008

FHT modification of SART

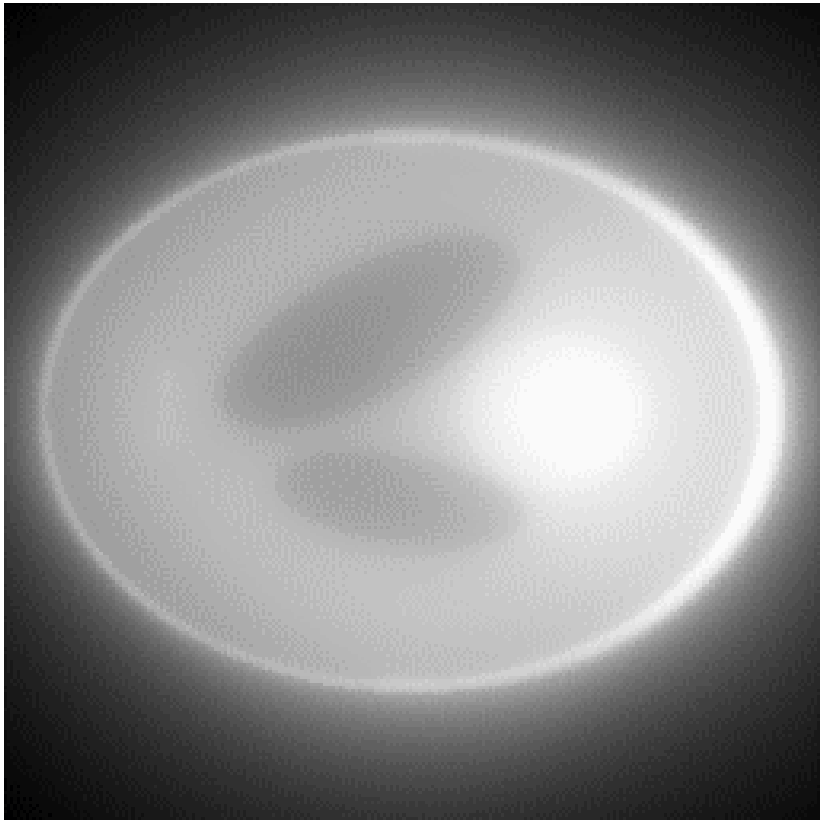

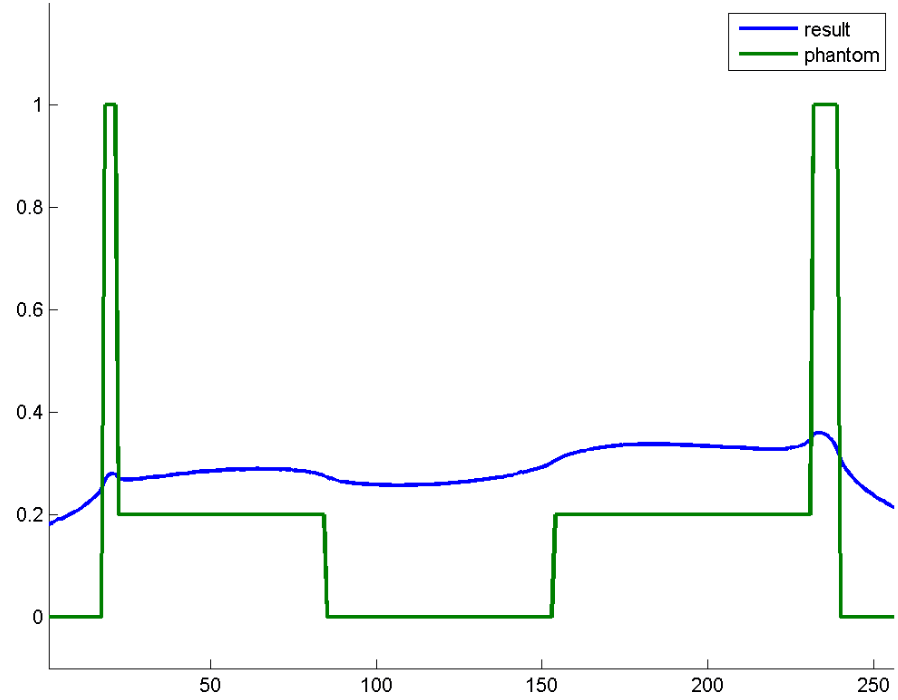

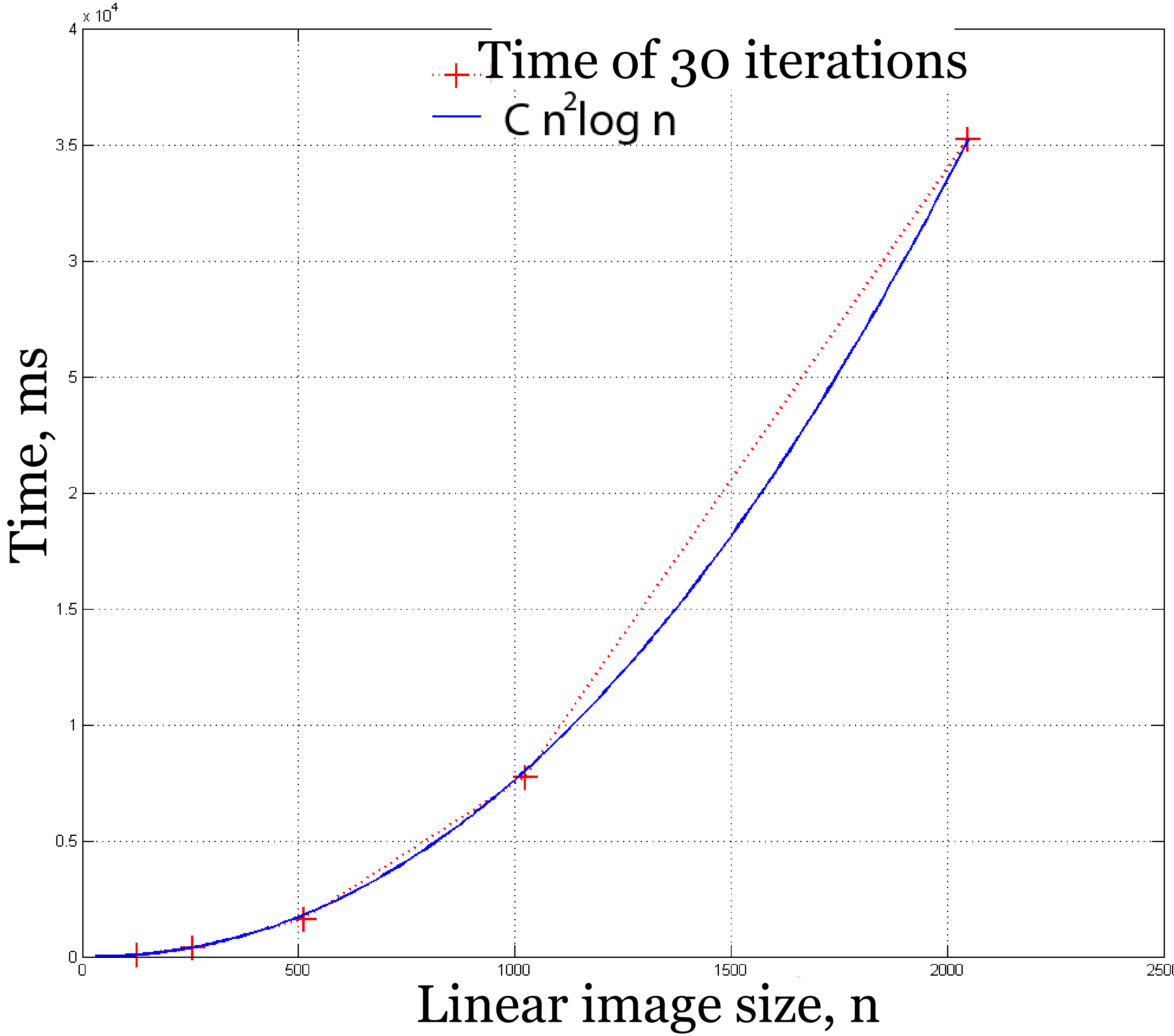

x 10^4
4
3.5
3
5
2
1.5
1
0.5
0
0
500
1000
1500
2000
2500
Time of 30 iterations
C n^2log n
Time, ms
Linear image size, n

A. Buzmakov,
V. Asadchikov, V. Proon
Shubnikov Institute of Crystallography RAS, Moscow, Russia

M. Chukalina,
Ya. Shabelnikova
Institute of Microelectronics Technology and High Purity Materials RAS, Chernogolovka, Russia

D. Nikolaev,
V. Sokolov,
S. Karpenko
Institute for Information Transmission Problems (Kharkevich Institute) RAS, Moscow, Russia

THANK YOU
FOR YOUR ATTENTION!

CORRECT ACCOUNTING OF ABSORPTION

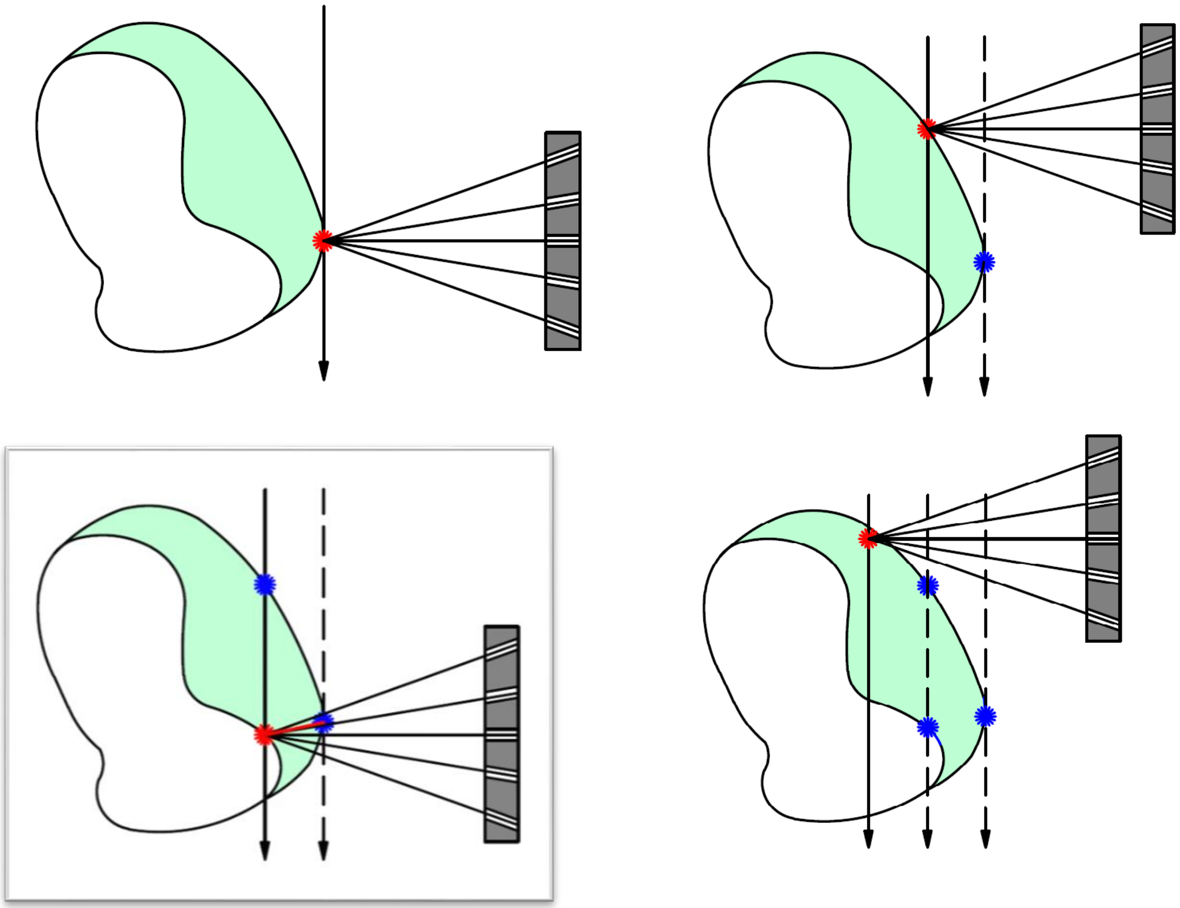

Solution: planar confocal collimator

OUTLINE

- Two different set-ups: tipical&confocal
- Confocal: two collimators geometry&properties
- Microbeam shape reconstruction: algorithms&schemes
- Fast core for calculations
- Multispectral visualization

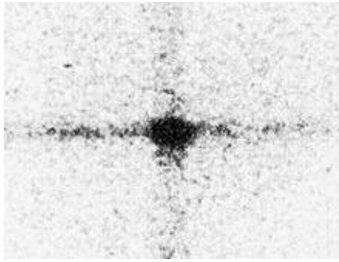

COMPLETE E-FIELD BEAM PROFILING

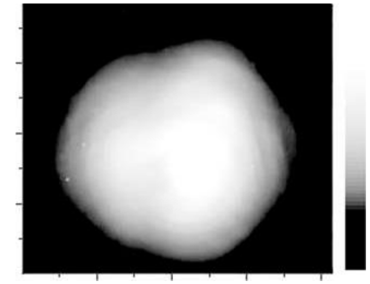

- **Scanning-aperture techniques**

  ✓Knife-edge technique or the scanning-slit profiler. By measuring the intensity curve in several directions, the original beam profile can be reconstructed using algorithms developed for x-ray tomography

  ✓high precision metal corner. By measuring the fluorescence curve in four scanning directions, the original beam profile can be reconstructed solving linear equations system

- **CCD camera technique**

SCANNING SCHEMES

- Choice of a metal corner is due to a simplicity of manufacturing technology

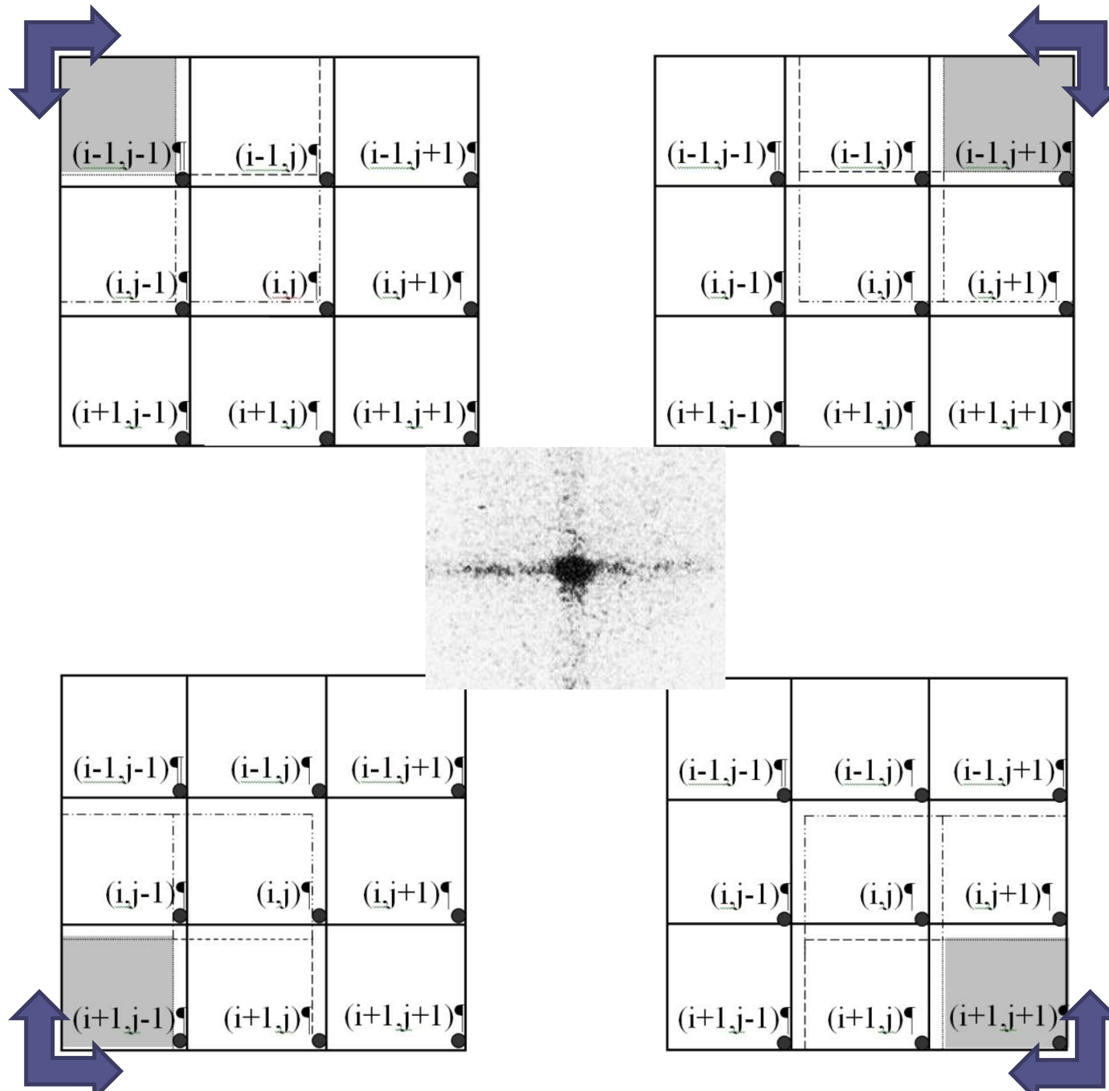

SIMULATION

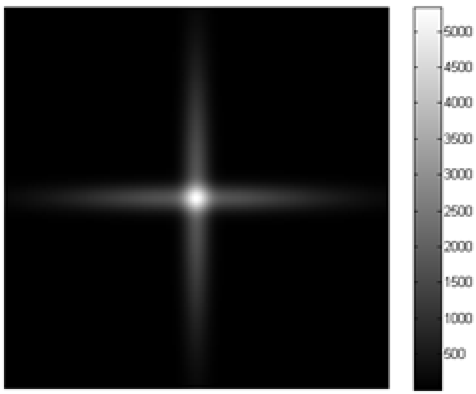

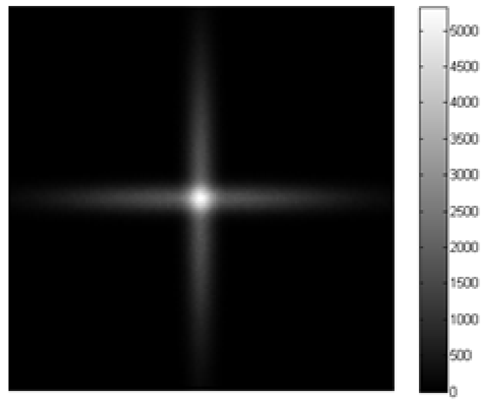

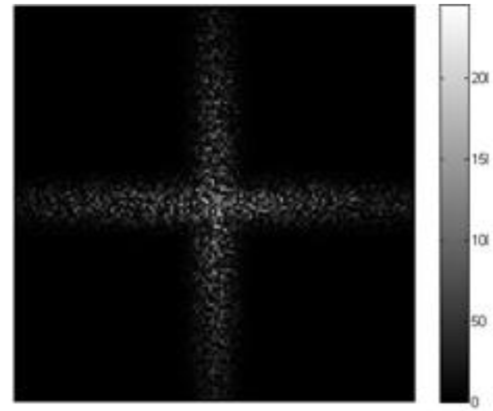

a) Ideal b) Ideal+Poisson c) b-a

d) Corner e)Collected signal f) Reconstructed

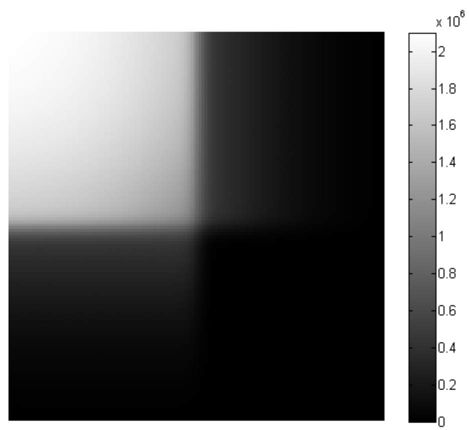

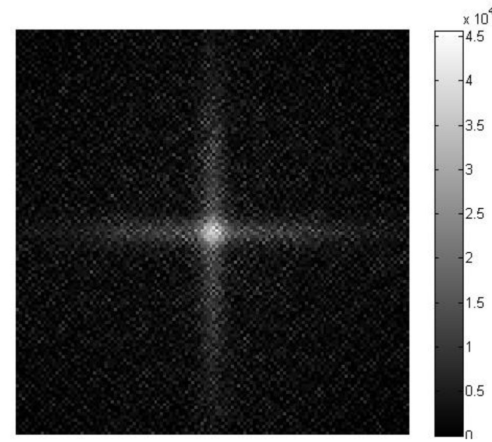

EXPERIMENT (X-ray lab source, IMT RAS)

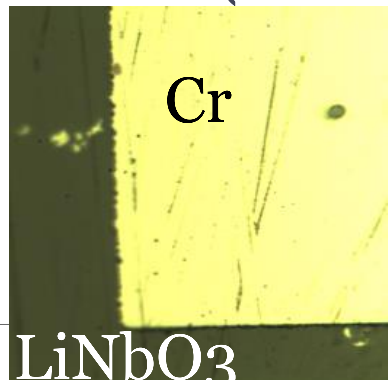

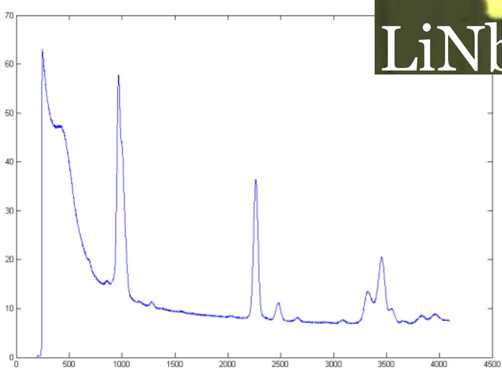

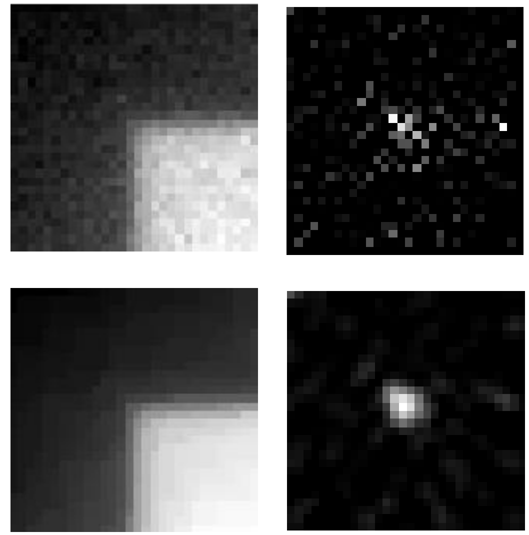

Preliminary experiment:
10 μm scanning step
1 min per step

Poisson property
average=variance

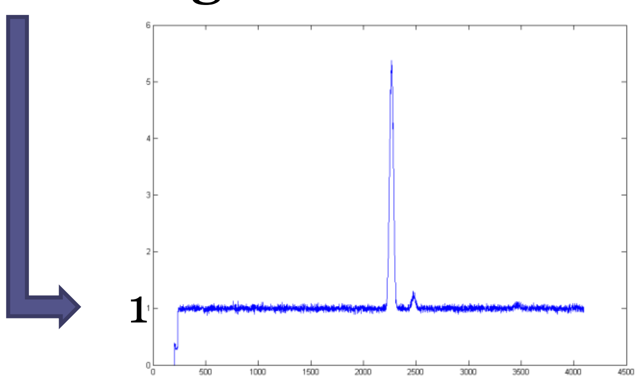

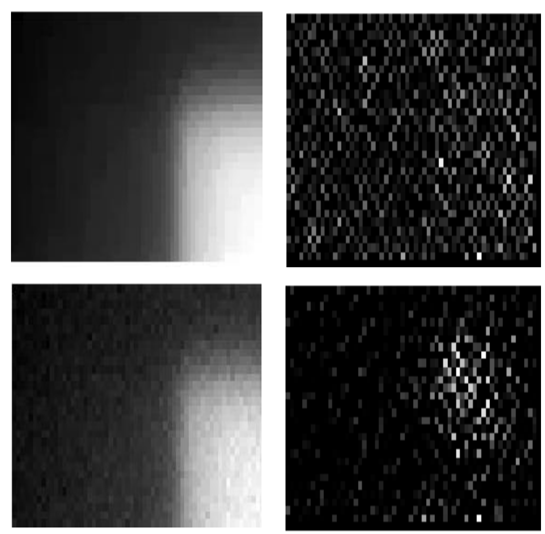

1 μm
scanning step

IMAGE PROCESSING

Linear system solution

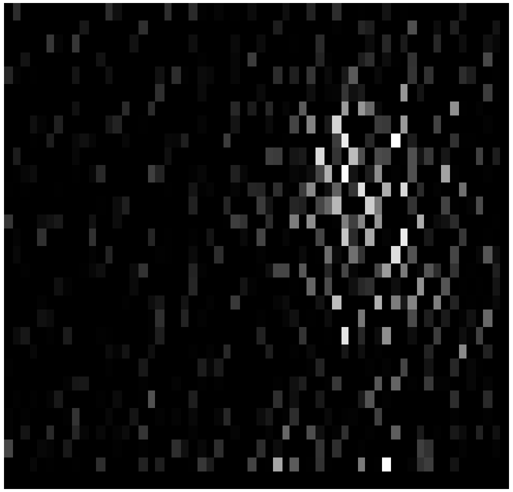

CCD camera

Nonlinear filtering technique for beam profile image enhancing

It uses a priory information about beam shape (radial monotonic decrease)

OUTLINE

- Two different set-ups: tipical&confocal
- Confocal: two collimators geometry&properties
- Microbeam shape reconstruction: algorithms&schemes
- Fast core for calculations
- Multispectral visualization

WHAT WE ARE DOING:

FBP

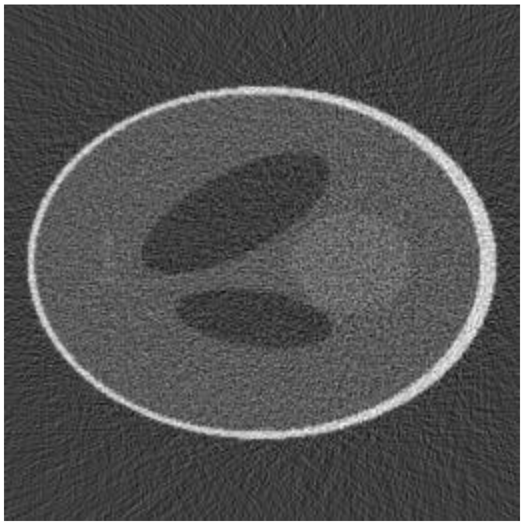

$O(n^2 \log n)$

SART

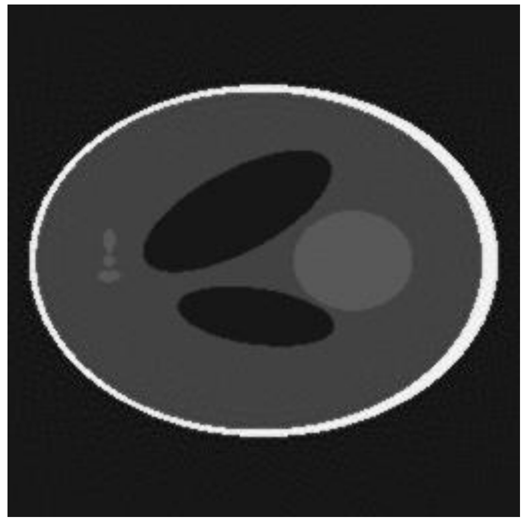

$O(n^3)$

SART + FHT

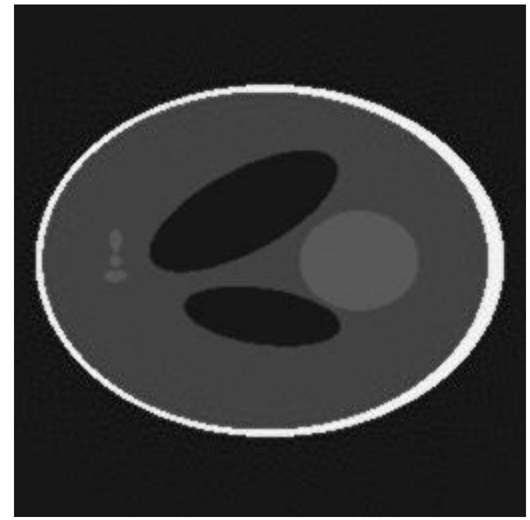

$O(n^2 \log n)$

FHT modification of SART

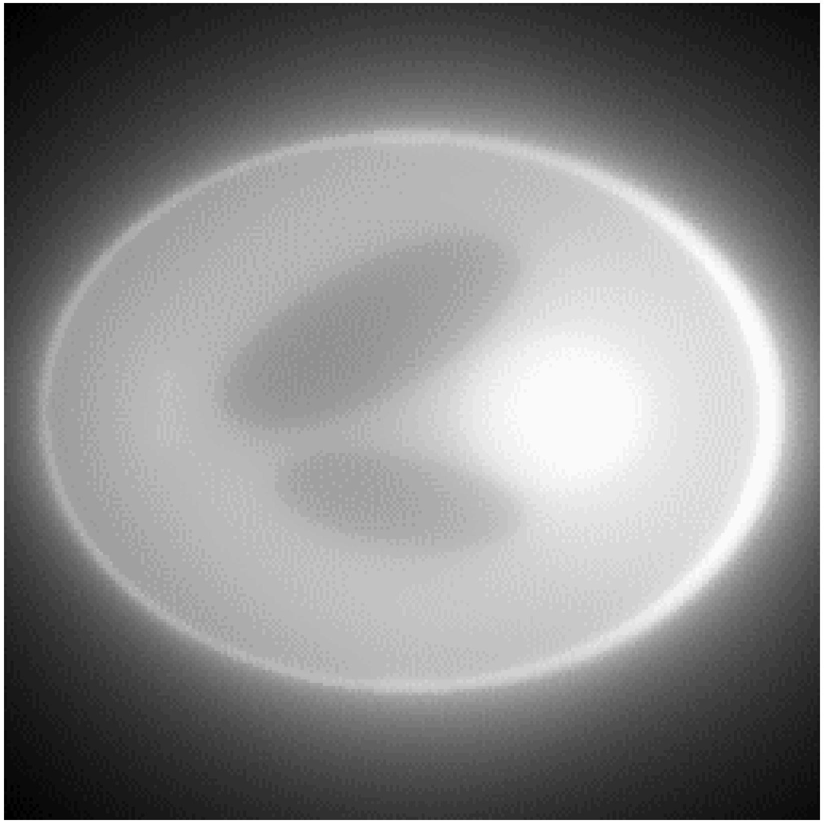

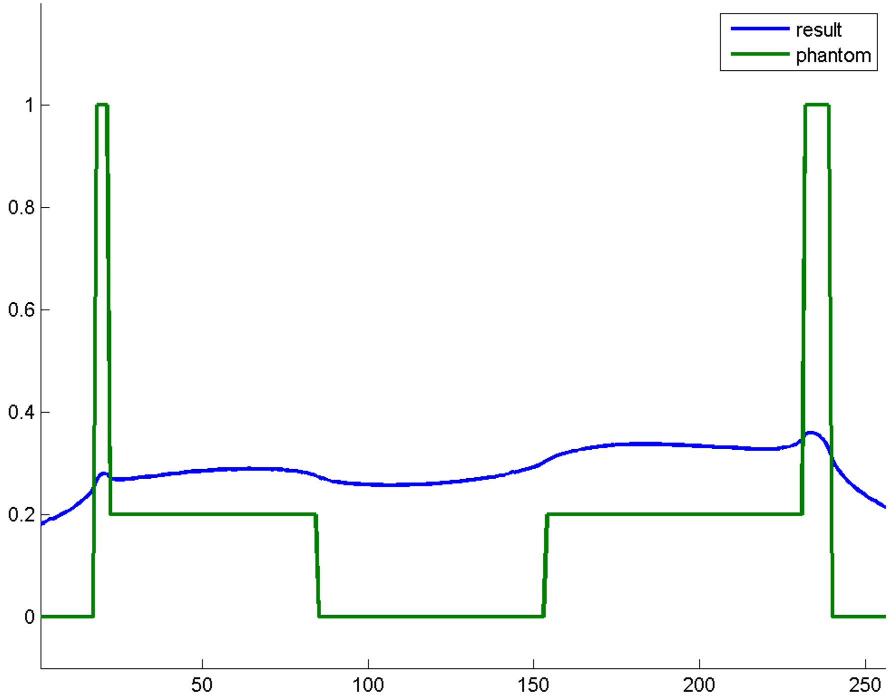

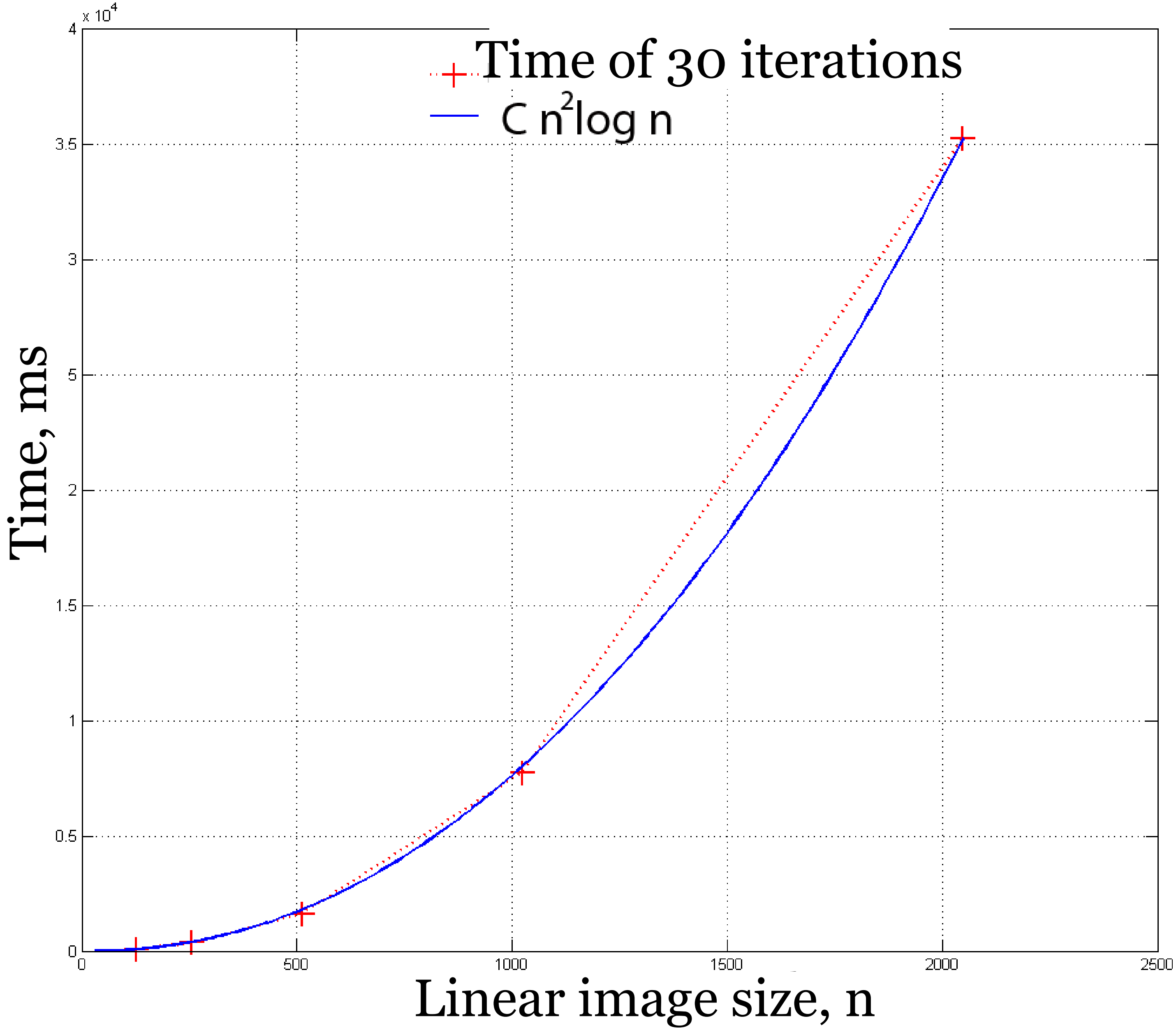

x 10^4
Time of 30 iterations
C n^2 log n
Time, ms
4
3.5
3
5
2
1.5
1
0.5
0
0
500
1000
1500
2000
2500
Linear image size, n

FAST HOUGH TRANSFORM

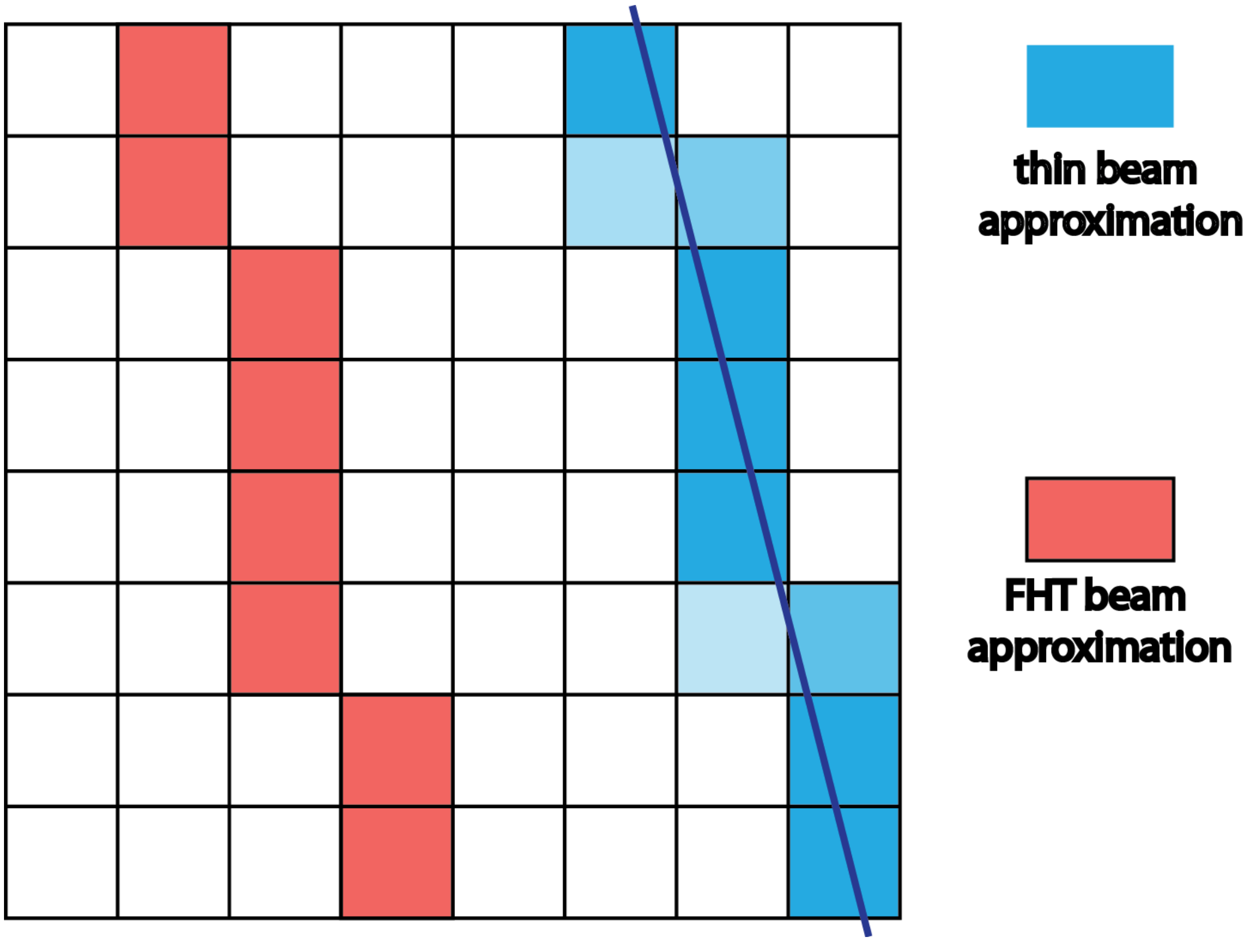

Number of different FHT angle patterns for nxn image ≈ 4n

FHT of an NxN image can be calculated with O(n^2log n) operations [3]

Nikolaev D., Karpenko S., Nikolaev I., Nikolayev P, 2008

SART iteration

$$f^{(k)} = f^{(k-1)} + \gamma \cdot W^T (p - Wf^{(k-1)})$$

Computational complexity of one iteration – $O(n^3)$

[2]

SART + FHT = $O(n^2 \log n)$ SART

Prun V., Buzmakov A., Nikolaev D., Chukalina M., Asadchikov V. “*Calculatively Effective Modification of ART in CT*”, Automation and Remote Control, In press, 2012.

FHT modification of SART

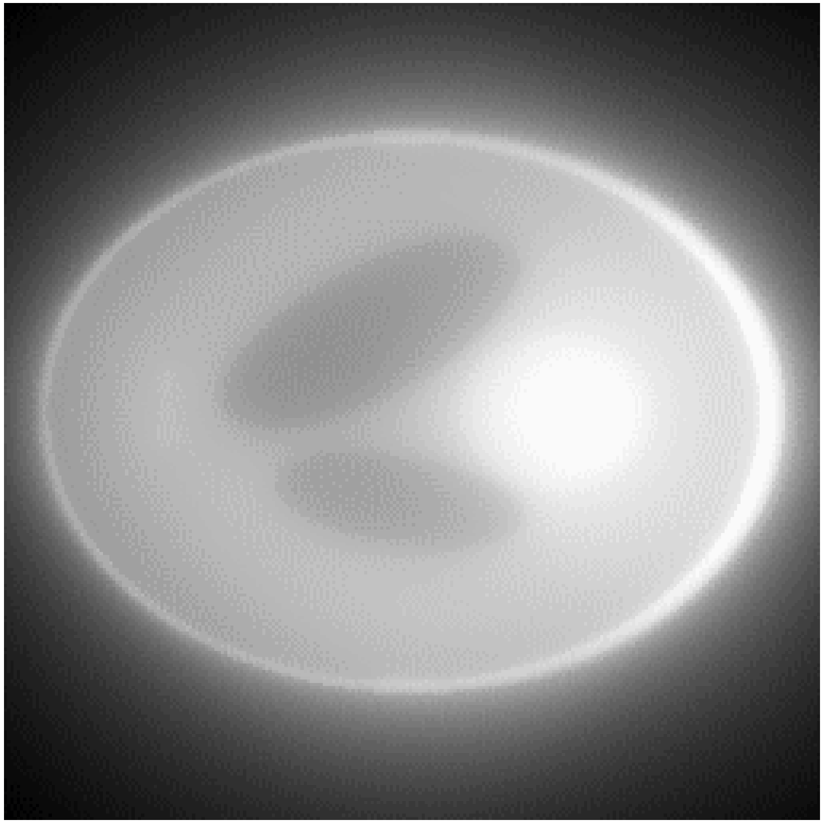

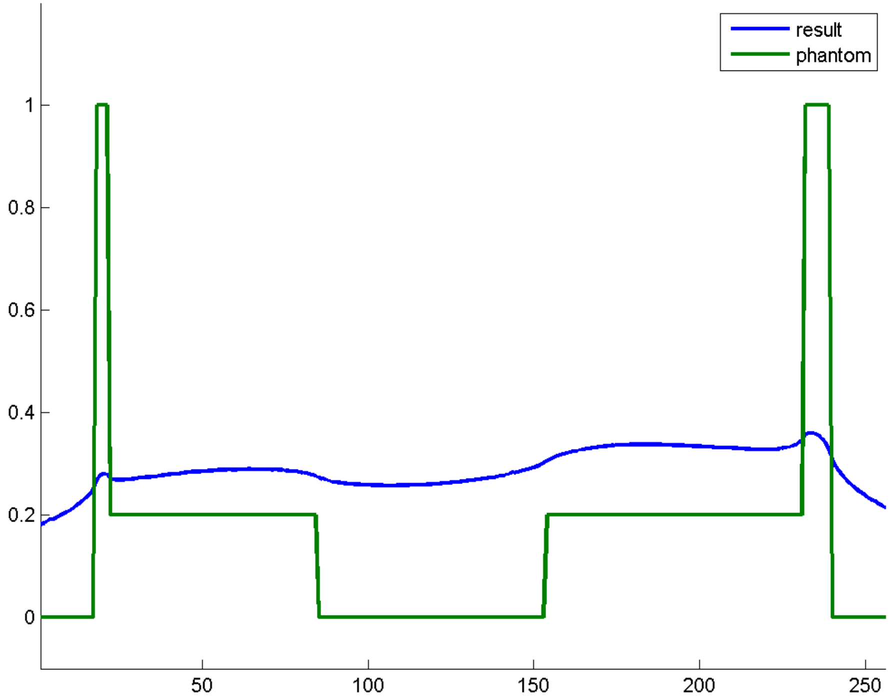

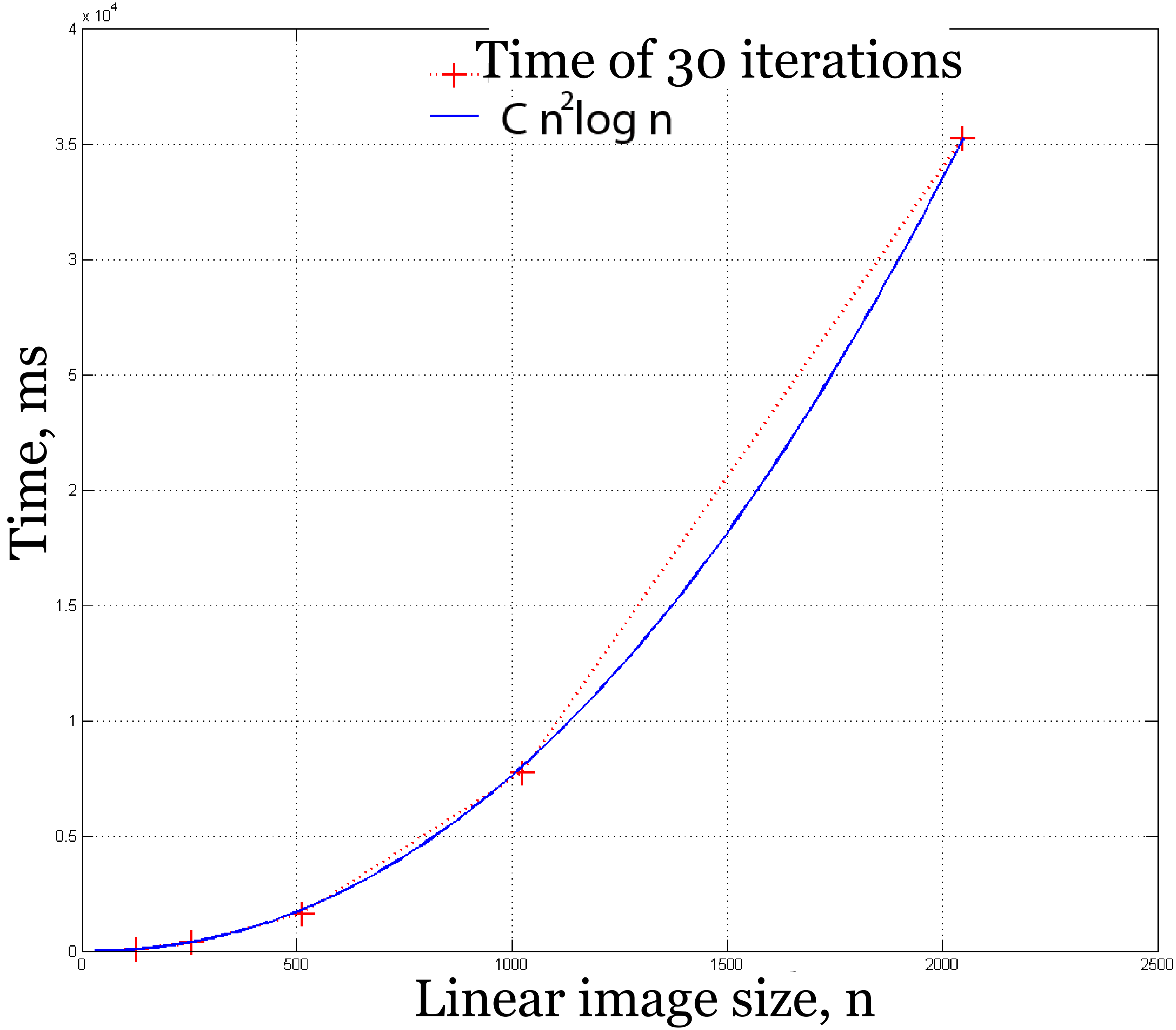

x 10^4
4
3.5
3
2.5
2
1.5
1
0.5
0
0
500
1000
1500
2000
2500
Time of 30 iterations
C n^2 log n
Time, ms
Linear image size, n

OUTLINE

- Two different set-ups: tipical&confocal
- Confocal: two collimators geometry&properties
- Microbeam shape reconstruction: algorithms&schemes
- Fast core for calculations
- Multispectral visualization

MATHEMATICAL ASPECTS

Multi-spectral image: vector function

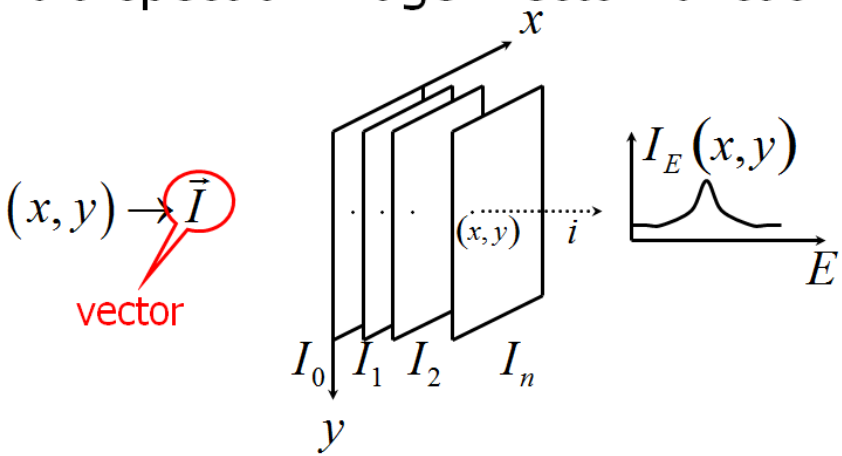

Grayscale image: scalar function

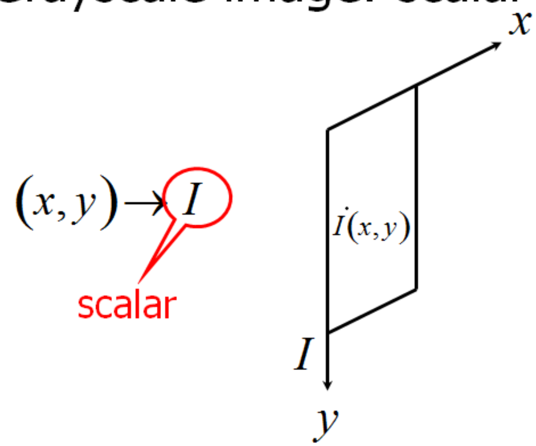

Object boundaries

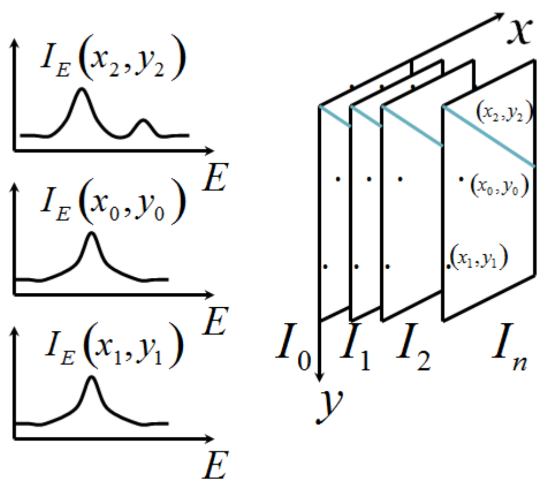

$$\frac{\left|\vec{I}(x_2,y_2)-\vec{I}(x_0,y_0)\right|}{\sqrt{(x_2-x_0)^2+(y_2-y_0)^2}} \gg \frac{\left|\vec{I}(x_1,y_1)-\vec{I}(x_0,y_0)\right|}{\sqrt{(x_1-x_0)^2+(y_1-y_0)^2}}$$

Sokolov et al, 2010, ISVC'10

MATHEMATICAL ASPECTS

We want to visualize the vector function while preserving all boundaries

$$T : \vec{I}(x, y) \to \tilde{I}(x, y)$$

$$\frac{\left|\vec{I}(x_2, y_2) - \vec{I}(x_0, y_0)\right|}{\sqrt{(x_2 - x_0)^2 + (y_2 - y_0)^2}} \gg \frac{\left|\vec{I}(x_1, y_1) - \vec{I}(x_0, y_0)\right|}{\sqrt{(x_1 - x_0)^2 + (y_1 - y_0)^2}} \Leftrightarrow \frac{\left|\tilde{I}(x_2, y_2) - \tilde{I}(x_0, y_0)\right|}{\sqrt{(x_2 - x_0)^2 + (y_2 - y_0)^2}} \gg \frac{\left|\tilde{I}(x_1, y_1) - \tilde{I}(x_0, y_0)\right|}{\sqrt{(x_1 - x_0)^2 + (y_1 - y_0)^2}}$$

$$\forall (x, y) : \overrightarrow{grad}\left(\vec{I}(x, y)\right) \approx \overrightarrow{grad}\left(\tilde{I}(x, y)\right)$$

MATHEMATICAL ASPECTS

- No gradient operator defined for vector fields
  - Use Di Zenzo color gradient

$$\vec{g} \leftarrow C\overrightarrow{grad}\left(\vec{I}\left(x,y\right)\right)$$

- Reconstruction by gradient have no exact solution
  - Use least squares best approximation

$$E_{sqr} = \left(\frac{\partial \tilde{I}\left(x,y\right)}{\partial x} - g_x\left(x,y\right)\right)^2 + \left(\frac{\partial \tilde{I}\left(x,y\right)}{\partial y} - g_y\left(x,y\right)\right)^2$$

$$\frac{\partial}{\partial x}\frac{\partial E}{\partial\left(\partial \tilde{I}/\partial x\right)} + \frac{\partial}{\partial y}\frac{\partial E}{\partial\left(\partial \tilde{I}/\partial y\right)} = 0$$

- Poisson's equation

$$\Delta \tilde{I}\left(x,y\right) = \partial g_x\left(x,y\right)/\partial x + \partial g_y\left(x,y\right)/\partial y$$

STRUCTURE VISUALIZATION

X-ray fluorescence scanning microscopy
1024-channel biological data (X-ray lab source, IC RAS)


Channel 256

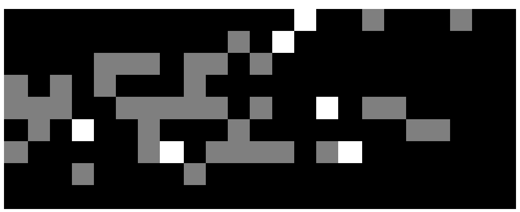
Channel 512

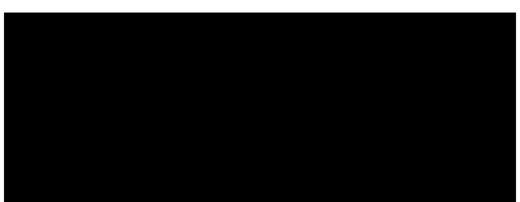
Channel 768

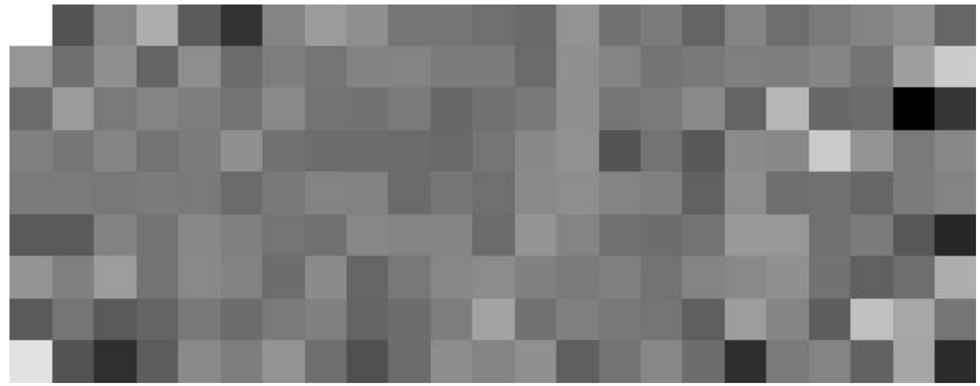
PCA visualization

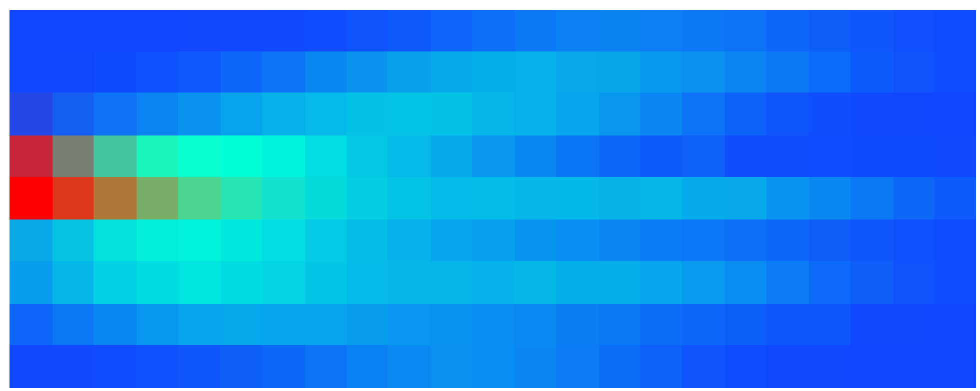
Structure visualization

CONCLUSIONS

- Two set-ups are used now but both wait for development of additional signal processing procedures:

  ✓Inverse problem solution for general case of classical experimental scheme

  ✓Inverse problem solution for signal correction with confocal cappillary set-up usage

- Decreasing of the beamsize asks for careful 2D beamshape reconstruction procedures